Marine Geology 378 (2016) 196–212

Contents lists available at ScienceDirect

Marine Geology

journal homepage: www.elsevier.com/locate/margo

Multidisciplinary study of mud volcanoes and diapirs and their relationship to seepages and bottom currents in the Gulf of Cádiz continental slope (northeastern sector)

Desirée Palomino [a,*], Nieves López-González [a], Juan-Tomás Vázquez [a], Luis-Miguel Fernández-Salas [b], José-Luis Rueda [a], Ricardo Sánchez-Leal [b], Víctor Díaz-del-Río [a]

[a] Instituto Español de Oceanografía, Centro Oceanográfico de Málaga, Puerto Pesquero S/N, 29640 Fuengirola, Málaga, Spain
[b] Instituto Español de Oceanografía, Centro Oceanográfico de Cádiz, Muelle Pesquero S/N, 11006 Cádiz, Spain

ARTICLE INFO

Article history:
Received 28 May 2015
Received in revised form 30 September 2015
Accepted 4 October 2015
Available online 9 October 2015

Keywords:
Seepage
Mud volcanoes
Diapirs
Benthic habitats
Bottom currents
Gulf of Cádiz

ABSTRACT

The seabed morphology, type of sediments, and dominant benthic species on eleven mud volcanoes and diapirs located on the northern sector of the Gulf of Cádiz continental slope have been studied. The morphological characteristics were grouped as: (i) fluid-escape-related features, (ii) bottom current features, (iii) mass movement features, (iv) tectonic features and (v) biogenic-related features. The dominant benthic species associated with fluid escape, hard substrates or soft bottoms, have also been mapped. A bottom current velocity analysis allowed, the morphological features to be correlated with the benthic habitats and the different sedimentary and oceanographic characteristics. The major factors controlling these features and the benthic habitats are mud flows and fluid-escape-related processes, as well as the interaction of deep water masses with the seafloor topography. Mud volcano eruptions give rise to mud flows and/or aqueous fluid seepage. These processes sustain chemosynthesis-based communities, closely associated with fluid seepage. Large depressions in the nearby area are influenced by collapse-related phenomena, where active fluid escape and the erosive effect of bottom currents have been identified. When the extrusion activity of the mud volcano is low and the seepage is diffuse, authigenic carbonates form within the edifice sediments. The bottom current sweeps the seafloor from the SE to the NW. When the velocity is moderate, sedimentary contourite processes take place on both sides of the edifices. At high velocities, the authigenic carbonates may be exhumed and colonised by species associated with hard substrates. Small carbonate mounds are found at the summits of some volcanoes and diapirs. Living corals have been found on the tops of the shallowest mud volcanoes, revealing different oceanographic conditions and strong bottom currents that favour the availability of nutrients and organic particles. The edifices affected by very high current velocities are located in the channels where erosive processes dominate.

1. Introduction

Mud diapirs and mud volcanoes (MVs) are very common structures on the middle and upper continental slope of the Gulf of Cádiz. Some mud diapirs build-up ridges or domes on the seafloor as the result of the slow uplift of massive plastic materials from the deep layers to the surface due to density differences. This gives rise to the deformation of the main linear structures on the continental slope of the Gulf of Cadiz (Fernández-Puga et al., 2007). In this area, upper Neogene–Quaternary tectonics has formed NE–NW thrusts that have favoured the rise of shale diapirs from the Neogene tectonics complex emplaced in the Gibraltar Arc front (Maldonado et al., 1999; Medialdea et al., 2004). When diapirs break through the seafloor, they form seafloor piercing structures, and usually they may have associated MV at top since they are formed by the vertical migration of muddy sediments and fluids (hydrocarbons and brines) that are extruded by successive emissions (Milkov, 2000). The main difference between a mud volcano and a mud diapir is that a mud volcano is characterised by actively extruding material while a mud diapir is form by a massive movement (Guliyev and Feizullayev, 1997; Milkov, 2000). Intermediate cases are the MV/diapir complexes that develop edifices of diapiric origin that harbour mud volcanoes at the surface and are generated as a consequence of fluid migration along the body of the diapir.

The Gulf of Cádiz has been extensively surveyed over recent decades. There are numerous studies focused on fluid emissions in MVs on both the Moroccan (Ivanov et al., 2000; Kenyon et al., 2000; Gardner, 2001; Van Rensbergen et al., 2005; León et al., 2012, and the references therein) and Iberian continental margins (Somoza et al., 2002, 2003; Díaz del Río et al., 2003; Pinheiro et al., 2003; Medialdea et al., 2009, and the references therein), as well as some studies on the benthic fauna associated with fluid migration and seepage (Rueda et al., 2012a; Cunha et al.,

* Corresponding author.
E-mail address: desiree.palomino@gmail.com (D. Palomino).

http://dx.doi.org/10.1016/j.margeo.2015.10.001
0025-3227/

2013; Rodrigues et al., 2013). In addition, many studies have looked at the Contourite Depositional System developed as a consequence of the interaction of the Mediterranean Outflow Water (MOW) with the continental margin (Gonthier et al., 1984; Faugères et al., 1985; Stow et al., 1986, 2002, 2013; Nelson et al., 1993, 1999; Schönfeld and Zahn, 2000; Llave et al., 2001, 2006, 2007, 2011; Mulder et al., 2002, 2003, 2006; Habgood et al., 2003; Hernández-Molina et al., 2003, 2006, 2011, 2014a,b), as well as the development of cold-water coral communities related to the contourite drifts (Van Rensbergen et al., 2005; Foubert et al., 2008; Wienberg et al., 2009). However, less attention has been paid to the relationship between the edifices and the recent geological and oceanographic processes, and the benthic communities and habitats that occur as a consequence of this interaction (Fernández Salas et al., 2012).

The edifices interact with the water masses, changing the water circulation pathways and velocities, and affecting the sedimentary processes in their vicinity (Davies and Laughton, 1972). This situation provokes a local circulation pattern that can support different habitats and associated benthic communities if both nutrient supply and substrate are adequate, and consequently a great variety of species is promoted (Cordes et al., 2010). Changes in oceanographic conditions can give rise to changes in the seabed morphology and habitats. Therefore, there is a strong relationship between deep water benthic communities, the water flow near the bottom, the type of substrate, and regional geological processes (Van Rooij et al., 2010; Fernández Salas et al., 2012).

The aim of this work is to study the seafloor morphology and the sub-surface characteristics of the MVs, diapirs and diapir/MV complexes on the Spanish continental margin of the Gulf of Cádiz; In addition, some of the structures are described here for the first time. This study enables us to understand the interaction of the volcanic edifices with the hydrodynamics of the water masses and the interplay between fluid escape, mud extrusion, mud diapirism, sediment dynamics, and their influence on the biosphere. We thus propose an evolutionary model for the MV, diapirs, and MV/diapir complexes with different developmental phases. This study has also contributed to the Spanish government's proposal to classify this area as a Site of Community Importance (ESZZ12002 Mud volcanoes of the Gulf of Cadiz) and include it in the European Union's Natura 2000 network.

2. Materials and methods

The data analysed in this study was obtained during five oceanographic cruises as part of the LIFE + INDEMARES/CHICA project in the area known as the Shallow Field of Fluid Expulsion (SFFE, Díaz del Río et al., 2014), which is located on the upper and middle slope of Gulf of Cádiz continental margin (Fig. 1B). The bathymetric data was acquired with a Kongsberg Simrad EM-710 multibeam echosounder (70 to 100 kHz) and processed with Caris Hips and Sips software to produce a 15 × 15 m bathymetric grid model. Backscatter values were also processed from swath bathymetry and morphological analyses were

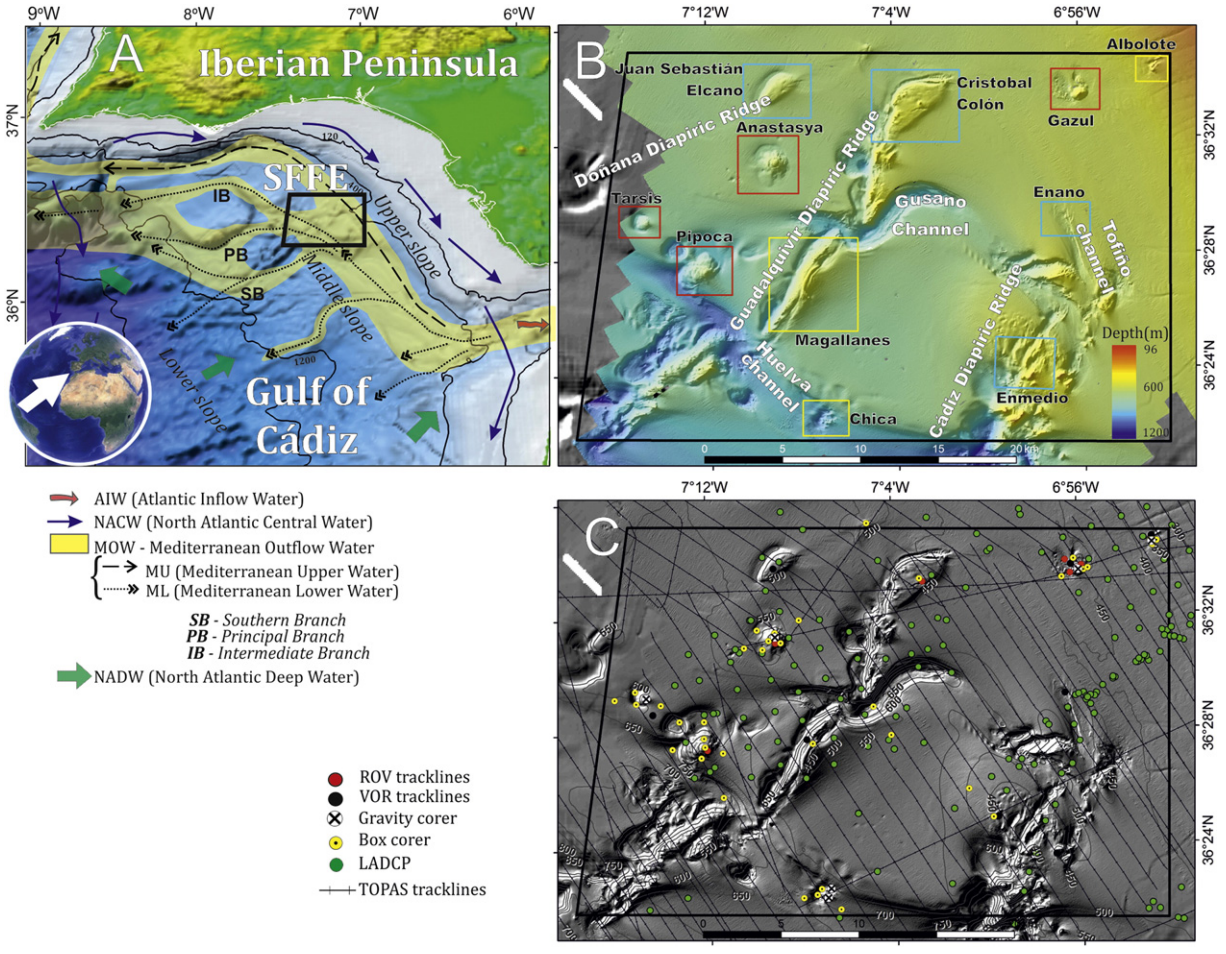

Fig. 1. A) Location of the Shallow Field of Fluid Expulsion (SFFE) in the middle slope of the Gulf of Cádiz indicating the study area (black polygon) and the regional water-mass circulation (modified by Hernández-Molina et al., 2003). The general bathymetric map was extracted from GEBCO (General Bathymetry Chart of the Oceans). B) Bathymetric map with a 15 × 15 m grid cell resolution showing the mud volcanoes (red polygons), diapirs (blue polygons) and MV/diapir complexes (yellow polygons) investigated in this study. C) Location of the samples and high-resolution seismic profile track lines. Detailed bathymetric maps are given in Figs. 2, 7 and 8.

conducted with the ArcGIS desktop software. Very high-resolution seismic profiles were acquired with the TOPAS PS018 (Topographic Parametric Sounding) system, working with a primary frequency from 16 to 20 kHz and a secondary frequency ranging from 0.5 to 4 kHz. Standard processing was applied during the acquisition: pre-amplifying, TVS amplifying and band-pass filtering. Seismic data were converted and imported as SEG-Y files into the IHS Kingdom software in order to interpret at the sedimentary units and their sub-surface characteristics.

Box-core samples were collected on selected MVs and diapirs, to characterise the sediment texture and faunal assemblages. Gravity cores were collected at the summits of the main features to confirm their nature. High-resolution pictures of the cores were acquired with an Avaatech XRF core scanner. High-resolution videos and images taken by the Remotely Operated Vehicle (ROV) LIROPUS 2000 and the Underwater Camara Sled (UCS) APHIA 2012 were used to map and identify benthic habitats and associated biota. Photographic and video observations were made with high precision underwater navigation, capturing images between 0.5 and 2.5 m from the seafloor, during 1–3 hour (ROV) and 0.6–1 hour (UCS) transects. The mean explored distances were between 223 and 1025 m for ROV transects and between 80 and 379 m for UCS transects. The underwater images were georeferenced using a transponder attached to the devices (ROV and UCS) plotted their position in relation to the research vessel during the transects. Near-bottom current speed measurements were carried out at several stations in the area, using a Lowered Acoustic Doppler Current Profiler (LADCP).

3. Geological and physiographical settings

The Gulf of Cádiz is situated towards the west of the Gibraltar Arc between the southwestern continental margin of the Iberian Peninsula and the northwestern continental margin of Africa (Fig. 1A). In this region, recent models have proposed the SWIM fault zone as the Africa–Eurasia plate boundary (Zitellini et al., 2009), connecting the Gorringe Bank and the Horseshoe Abyssal Plain to the west and the Rif System to the east. In this area an incipient subduction zone of the Atlantic oceanic crust beneath Iberia may be forming (Duarte et al., 2013). The geodynamic evolution of the area from the Eocene is characterised by successive phases of compressive to oblique regimes trending from N–S to NW–SE (Maldonado et al., 1999). The westward drift of the Alboran Crustal Domain and its collision with the continental margins of the African and Eurasian plates, occurring from the upper Oligocene to the Tortonian, gave rise to the maximum compression related to the Betic-Rif compressive belt and the emplacement at their front of the Allochthonous Unit of the Gulf of Cádiz (AUGC) as an accretionary wedge (Flinch et al., 1996; Maldonado et al., 1999; Medialdea et al., 2004; Platt et al., 2013). From the Upper Tortonian the compression regime drifts to a WNW–ESE compression (Dewey et al., 1989). Post-Tortonian regional reorganisation induced the extensional collapse westwards of the AUGC by NW–SE trending extensional faults, tectonic subsidence and strong diapiric processes (Flinch et al., 1996; Somoza et al., 1999; Gracia et al., 2003; Maestro et al., 2003; Medialdea et al., 2004; Fernández-Puga et al., 2007). The emplacement of NE–SW diapiric ridges along thrust faults takes advantage of transfer faults linking the extensional systems (Maestro et al., 2003; Fernández-Puga et al., 2007). The diapiric structures are mainly rooted in the AUGC and comprise by Late Triassic to Lower Jurassic evaporite units (Matias et al., 2011), as well as a melange of Upper Cretaceous–Palaeogene deep-water sedimentary rocks to Miocene marls (Flinch et al., 1996). The migration of these shale and evaporitic units triggered diapiric processes that developed as isolated morphological highs and ridge systems. Diapirism and related tectonics provide adequate gas migration pathways along the normal fault system that facilitates the generation of MV. At the end of the Lower Pliocene subsidence decreased, and the margin evolved towards a stable phase during the Upper Pliocene–Quaternary (Nelson et al., 1993; Maldonado et al., 1999; Somoza et al., 1999; Maestro et al., 2003; Medialdea et al., 2004, 2009). However, Quaternary uplift and reactivation of several diapiric structures along the Gulf of Cadiz margin have been proven by high-resolution seismics (Fernández Puga et al., 2010, 2014; Vázquez et al., 2010).

The continental slope of the Gulf of Cádiz has traditionally been divided into three domains (Heezen and Johnson, 1969; Maldonado and Nelson, 1999). The upper slope extends from 120 to 400 m water depth with a slope angle of 1.3°. The middle slope is situated between 400 and 1200 m water depth, and has a lower mean slope angle (0.38°) than the upper slope. The lower slope extends from 1200 m to 2000 water depth and has a mean slope angle of 0.8°.

The SFFE occurs from water depths of 300 to 730 m, and the main reliefs and associated features are located on the middle slope, with the exception of the Albolote complex which is located at 386 m water depth on the upper slope. The study area encompasses mainly channels and ridges, according to the terminology proposed by Hernández-Molina et al. (2006) for the middle slope of the continental margin of the Gulf of Cádiz. It is characterised by the presence of two main diapiric ridges: the Guadalquivir Diapir Ridge (GDR) with a NE–SW direction and the Cádiz Diapiric Ridge (CDR). In this area there are also buried or quasi-buried diapiric ridges, such as the Doñana Diapiric Ridge to the north of the GDR (Fig. 1) (Somoza et al., 2003; Fernández-Puga et al., 2007). In addition, two main contourite channels with sinuous morphology are present in this zone: the Gusano and Huelva channels (García et al., 2009). These channels flow through the SFFE in E–W and SE–NW directions respectively. The smaller NNW–SSE oriented Tofiño channel, is located to the north of the CDR (Fig. 1). The upper slope is crossed by turbidite channels with a predominantly ENE–WSW direction that reach the shallowest part of the study area in the NE (Rodero et al., 2000; Díaz del Río et al., 2012). All these features are emplaced over relict contourite deposits (Hernández-Molina et al., 2006), and are affected by tectonics and diapiric processes that favour the formation of characteristic edifices such as MVs, mud diapirs and the MV/diapir complexes. Previously, the Anastasya and Pipoca MVs had been reported and their MV nature confirmed (Somoza et al., 2003; Martín-Puertas et al., 2007), but in this study five new MVs and MV/diapir complexes (Tarsis, Albolote, Gazul, Chica and Magallanes) have been confirmed based on the presence of mud breccias in gravity cores.

4. Oceanographic settings

The oceanographic circulation in the Gulf of Cádiz is controlled by the exchange of water masses through the Strait of Gibraltar, the surficial Atlantic Water (AIW) flows into the Alboran Sea, and the deeper Mediterranean Outflow Water (MOW) flows out to the Atlantic Ocean (Lacombe and Lizeray, 1959; Ochoa and Bray, 1991; Nelson et al., 1999). The MOW sweeps the Iberian margin as a seafloor bottom current from 400 m to 1200 m water depth (36.1–36.9 psu and ca. 13 °C), and it is intercalated below the North Atlantic Central Water (NACW; 35.6–36.5 psu and 11–17 °C) and above the North Atlantic Deep Water (NADW; 34.9–35.2 psu and 3–8 °C) (Lacombe and Lizeray, 1959; Zenk, 1975; Thorpe, 1976; Ochoa and Bray, 1991; Ambar et al., 1999; Serra et al., 2005). The MOW flows to the north and west due to the Coriolis deflection and is separated into two main cores: a Mediterranean Upper Core (MU) and a Mediterranean Lower Core (ML) (Madelain, 1970; Ambar and Howe, 1979). At longitude 7°W, the ML divides into three well-defined branches (Madelain, 1970; Zenk, 1975; Ambar and Howe, 1979; Johnson and Stevens, 2000; Borenäs et al., 2002). The intermediate branch flows between 700 and 900 m water depth to the NW through the Diego Cao channel. The principal branch of the MOW, flowing between 900 and 1000 m water depth, is highly influenced by the seafloor topography and flows through the Cádiz Contourite Channel and south of the Cádiz Diapiric Ridge. The southern branch flows between 1000 and 1200 m water depth as an intermediate water mass, with a cyclonic gyre into the Gulf of Cádiz (Fig. 1). Recently, a water mass of modified Antarctic Atlantic Intermediate Water (AAIW) was identified in the Gulf of Cadiz flowing

to the NW (Louarn and Morin, 2011). This water mass has even been recorded in the eastern area of the Gulf of Cadiz (Hernández-Molina et al., 2014a) where it represents the coldest water mass above the lower branches of the MOW (bottom boundary down to 600–625 m). These authors propose that the AAIW confines the MOW and NACW against the slope.

Therefore, the study area is influenced by the ENACW and the MU branch of the MOW. Sánchez and Relvas (2003) adopted the water depth of 400 m as the reference level for the interface between the ENACW and the MOW near the Strait of Gibraltar, although in the study zone, this interface is located at a depth of 450–550 m (Fernández Salas et al., 2012). Since the MOW and the ENACW flow in opposite directions, the velocity of the interface would be near zero (Criado-Aldeanueva et al., 2006).

These bottom currents reach a maximum speed of 0.3–0.5 m/s along the contourite channels (Guadalquivir, Gusano and Tofiño), in contrast to the minimum speeds of between 0.01–0.1 m/s that are observed in the zone between the ridges (GDR and CDR) and between Anastasya MV and Gusano Channel (Fernández Salas et al., 2012; Díaz del Río et al., 2014).

5. Results

In the SFFE on the Gulf of Cádiz Spanish margin, three types of seafloor edifices linked to fluid emissions were differentiated according to their morphological characteristics and the nature of the extruded material. These three types are: mud volcanoes, mud diapirs and MV/diapir complexes (Fig. 1). Their dimensions and morphological characteristics are summarised in Table 1. The abundance of dominant macrofaunal species is summarised in Table 2.

Four mud volcanoes were studied: Gazul, Anastasya, Pipoca and Tarsis. All display a single cone with a fairly subcircular shape in plan view. They show evidence of mud breccia extrusion and their mud volcanic nature was confirmed by coring. Four mud diapirs were also observed: Cristóbal Colón, Juan Sebastián Elcano, Enano, and Enmedio. Three MV/diapir complexes were identified: Albolote, Chica, and Magallanes. These complexes appear as an uplift of the surface but their shapes comprise several mud volcano cones. All the MV/diapir complexes have evidence of mud breccia deposits that confirms the mud volcano character of these structures.

5.1. Mud volcanoes

5.1.1. Gazul MV

Gazul MV is located in the NW of the SFFE and to the north of the Cádiz diapiric ridge (Fig. 1B). It is the shallowest mud volcano in the study area, located at about 360 m water depth. It presents a subcircular base and an asymmetrical bathymetric profile, with flanks of different lengths oriented NE–SW. The summit stands at a water depth of 363 m and has a maximum height of 107 m. This MV has two prolongations or spurs running NW–SE that are interpreted as outcrops of muddy materials surrounded by two depressions. These outcrops are 40 and 22 m in height and they have high backscatter values (−22 to −25 dB). Both associated depressions are located north and northwest of the MV: they are 15 and 20 m deep and reach lengths of 2.1 and 2.3 km, respectively. A series of elevations about 55 m wide occur to the west of the western depression, at depths of between 460 and 480 m (Fig. 2a). These elevations either occur as isolated mounds, rounded or elongated in shape, or are grouped, giving rise to crests or ridges that can reach lengths of 650 m; they are principally oriented NW–SE and have higher backscatter values than the surrounding zones (Fig. 2e). This zone of ridges and mounds shows, in very high-resolution seismics, a high amplitude reflector at the seafloor surface that is interrupted as diffractions corresponding to the mounds (Fig. 2i). The internal structure is not discernible although parallel reflectors do appear truncated against the mounds. Sediment samples collected in the zone of the mounds indicate that the high backscatter values correspond to authigenic carbonate, mainly slabs and chimneys, which are colonised by abundant sessile fauna, mainly sponges.

A 42 cm long gravity core (TG07) was recovered from the summit of this MV at a water depth of at 364 m (Fig. 3). The material recovered comprised a millimetric layer of hemipelagic mud sediments at the top of the core followed by greenish grey mud breccia facies with abundant clasts. In general, the sediments at the summit contained a large number of bioclasts and authigenic carbonates. Subfossil remains of valves from the bivalve *Lucinoma asapheus* were retrieved in box-core samples, as well as few individuals of *Siboglinum* sp. Seabed video and ROV observations showed that at the summit the sandy-mud sediments are colonised by pennatulaceans. On the north and northwestern flanks, the substrate is mainly colonised by living cold-water corals (*Madrepora oculata* and *Lophelia pertusa*) and several species of gorgonians and anthipatharians. In the SW depression, the sediment is coarser and composed of sand and gravel, and is dominated by solitary corals (*Flabellum chunii*) and echinoids (*Cidaris cidaris*) (Fig. 4).

5.1.2. Anastasya MV

Anastasya MV is located to the northwest of the Guadalquivir diapiric ridge and to the north of the Gusano channel (Fig. 1). It presents a sub-circular basal shape with a slightly asymmetric bathymetric profile, with about 20 m of depth difference between the northern and southern sides at the base of the edifice. The Anastasya MV is located at a mean depth of 567 m (Fig. 2b). The water depth at the summit is located at 457 m and comprises a well-developed main cone of dome-like morphology. This dome is surrounded by a surface with a lower slope angle that gives rise to a depression 200 m wide and 12 m deep to the west, and to terracing at 490 m to the east, the surface of which is tilted to the W (Fig. 2j). Mud flows and gullies are observed along the flanks, crossing the MV from the summit to the base of the edifice, and there are also four slide scars on the southeastern flank (Fig. 2f). The very high-resolution seismic profiles show a subparallel sea bottom reflector along the flanks of the MV, defining the base of a transparent unit. Truncated reflectors are observed down the western side at the edges of the

Table 1
Location and morphological parameters of the MVs, diapir and MV/diapir complexes of the SFFE. Maximum and minimum lengths have been measured as the longest and shortest axes along the edifices. Heights have been measured as the distance from the shallowest depth of each edifice to the adjacent sea bottom.

Name	Type	Location	Max./min. depth (m)	Max./min. length (km)	Height (m)	Area (km^2)	Max./min. slope (°)
Gazul	Mud volcano	36°33.53′N/6°55.96′W	470/363	1.12/0.84	107	0.75	0.5/25
Anastasya	Mud volcano	36°31.34′N/7°9.07′W	555/457	2.3/1.8	98	3.26	0.3/23
Pipoca	Mud volcano	36°27.57′N/7°12.15′W	762/503	2.89/1.1	200–115	4.54	0.5/25
Tarsis	Mud volcano	36°29.29′N/7°14.67′W	680–585/550	1.5/0.9	130–35	1.02	0.3/20
Cristóbal Colón	Diapir	36°33.31′N/7°2.81′W	525/389	5.5/2.5	136–65	9.7	0.2/34
Juan Sebastián Elcano	Diapir	36°33.97′N/7°8.74′W	556/462	3/1.5	94–57	3.8	0.1/16
Enano	Diapir	36° 28.29′N/6°56.52′W	490/458	0.8/0.5	32	0.4	1.5/24
Enmedio	Diapir	36° 25.18′N/6°59.49′W	490/433	2.5/2.3	10	4	0.1/22
Albolote	Diapir/MV complex	36°34.47′N/6°52.74′W	386/328	1.25/1.03	58	1.06	0.5/25
Chica	Diapir/MV complex	36°22.34′N/7°6.87′W	759/652	1.5/1	40	1.9	0.5/30
Magallanes	Diapir/MV complex	36°27.19′N/7°7.88′W	601/407	7.8/2	194–113	14.6	0.4/38

Table 2
Abundance of dominant macrofaunal species found in box-core samples as well as in ROV and UCS transects performed in different mud volcanoes and diapirs of the Spanish Margin of the Gulf of Cádiz. Ind: Individuals; Col: Colonies.

Name	Box-Corer	ROV	USC
Gazul	*Siboglinum* sp. (11 ind. m^{-2}) *Lucinoma asapheus* (2 shell remains)	*Madrepora oculata* (4–10 col. m^{-2}) *Lophelia pertusa* (<1 col. m^{-2}) *Flabellum chunii* (1–2 ind. m^{-2}) *Cidaris cidaris* (1–2 ind. m^{-2})	
Anastasya	Siboglinum sp. (264 indiv. m^{-2}) *L. asapheus* (22 ind. m^{-2}) *Solemya elarraichensis* (66.7 ind. m^{-2}) *Calliax* sp. (132 ind. m^{-2})	*Funiculina quadrangularis* (<1 col. m^{-2}) *Kophobelemnon stelliferum* (2–5 col. m^{-2}) Bacterial mats (<5 bacterial mats. m^{-2})	
Pipoca	*Siboglinum* sp. (77 ind. m^{-2}) *Calliax* sp. (44 ind. m^{-2}) *L. asapheus* (1 shell remain)	*Leptometra phalangium* (40–80 ind. m^{-2}) *Flabellum chunii* (1–2 ind. m^{-2})	
Tarsis	*Siboglinum* sp. (11 ind. m^{-2}) *Calliax* sp. (11 ind. m^{-2})		*Leptometra phalangium* (5–10 col. m^{-2}) *Funiculina quadrangularis* (1–2 col. m^{-2}) *Kophobelemnon stelliferum* (10–15 col. m^{-2}) *Thenea muricata* (1–2 col. m^{-2})
Cristóbal Colón	Abundant coral remains (*M. oculata*, *L. pertusa*)	*Bebryce mollis*, *Switia pallida*, *Placogorgia* sp. (2–8 col. m^{-2}) *F. quadrangularis*, *Pennatula aculeata*, *K. stelliferum* (1–5 col. m^{-2})	
Juan Sebastián Elcano			*K. stelliferum*, *P. aculeata*, *F. quadrangularis* (1–5 col. m^{-2})
Enano			*Leiopathes glaberrima* (1–2 col. m^{-2}) *C. cidaris*, *Echinus* sp. (<1–1 ind. m^{-2}) *Charonia lampas* (<1 ind. m^{-2}) *T. muricata* (1–2 col. m^{-2})
Enmedio	Abundant coral remains (*M. oculata*, *Stenocyathus vermiformis*)		*F. quadrangularis*, *K. stelliferum* (4–9 col. m^{-2}) *T. muricata* (1–2 col. m^{-2}) *Asconema setubalense*, *Phakellia* sp., *Petrosia* cf. *crassa* (1–5 col. m^{-2}) *Callogorgia verticillata* (<1–1 col. m^{-2}) *Neocomatella europaea* (4–8 ind. m^{-2}) *Helycolenus dactylopterus* (<1 ind. m^{-2})
Albolote	Abundant coral remains (*M. oculata*, *L. pertusa*, *D. cornigera*) *Lucinoma asapheus* (2 shell remains) *Lytocarpia*, *Acryptolaria*, *Sertularella* (55 col. m^{-2}) *Bebryce mollis*, *Swiftia pallida* (22 col. m^{-2}) *Anthomastus* sp. (11 col. m^{-2})		*C. cidaris* (<1–1 ind. m^{-2}) *Munida* sp. (2–5 ind. m^{-2})
Chica			*C. verticillata*, *L. glaberrima* (1–2 col. m^{-2}) *A. setubalense*, *P.* cf. *crassa* (2–3 col. m^{-2})
Magallanes			*L. phalangium* (40–50 ind. m^{-2}) *F. chunii* (1–2 col. m^{-2}) *G. vitreus* (1–2 ind. m^{-2}) *H. dactylopterus*, *Chlorophtalmus agassizi* (<1 ind. m^{-2})

depression. To the west of the MV moat, the sedimentary units are folded, into a slightly domed anticline with normal faulting to the west. The average depth of the moat is about 20 to 25 m and the seismic facies are mainly transparent. Nine pockmarks are observed in the vicinity of the Anastasya MV, two of them being located to the north and the rest grouped to the west-southwest of the main edifice (Figs. 5 and 2b). In general, these pockmarks are circular in shape, although they are sometimes oval. In the seismic profiles, these pockmarks seem to be associated with normal faults that can reach the seafloor surface. Backscatter values are constant along the volcano and there is no significant difference with the surrounding areas (Fig. 2f).

A 52 cm-long gravity core (TG08) was recovered from the summit of the MV at 457 m water depth. It is characterised by mud breccia facies with a mousse-like texture as consequence of the high gas saturation, and it smells strongly of hydrogen sulphide. The top 19 cm of the core shows interbedded layers of hemipelagic and mud breccia sediments (Fig. 3). One of the most remarkable characteristics at the summit of Anastasya MV is the presence of bacterial mats, 25 cm in diameter, which were observed on ROV images (Fig. 4a). The benthic fauna is dominated by chemosymbiotic species linked to muddy sediments from cold seeps with moderate emissions. The most noteworthy species occurring at the summit are the polychaetes *Siboglinum* sp., the decapod *Calliax* sp., and the bivalves *L. asapheus* and *Solemya elarraichensis* (Fig. 4).

5.1.3. Pipoca MV

Pipoca mud volcano is located to the west of the Guadalquivir diapiric ridge and to the north of the Huelva channel (Fig. 1). It is sub-conical in shape and has an elliptical base. The major semi-axis (ENE–WSW) is 2.89 km and the minor one of 1.1 km. It has an asymmetrical bathymetric profile, with flanks of different lengths. The summit is dome-shaped and stands at a water depth of 503 m. A large mud flow, characterised by high backscatter values (−23 to −24 dB), runs from the summit down to 762 m water depth, crossing the mud volcano edifice southwestward and interrupting the Huelva channel (Fig. 2c, g). On the mud flow surfaces, several superimposed lobes have been imaged by multibeam bathymetry. The edifice is characterised to the southeast by plastered contourite deposits that overlap the volcano flank. Some slide scars can be seen at the contourite-volcano limit. Very high-resolution seismic profiles reveal chaotic-to-transparent units interpreted as mud flows with faults that also interrupt the contourite deposits. The mud flows are buried between sedimentary layers of sub-parallel reflectors (Fig. 2l). Two large depressions, with areas of ca. 2 and 5 km^2 respectively, are located to the northeast and northwest of the volcano. The depression to the northeast is irregular in shape and filled by sediments 18 m thick. The depression in the northwest is sub-circular in plan view with edges that have almost vertical walls which end on a low-gradient flat-bottomed surface. The bottom of the smaller depression is slightly tilted to the

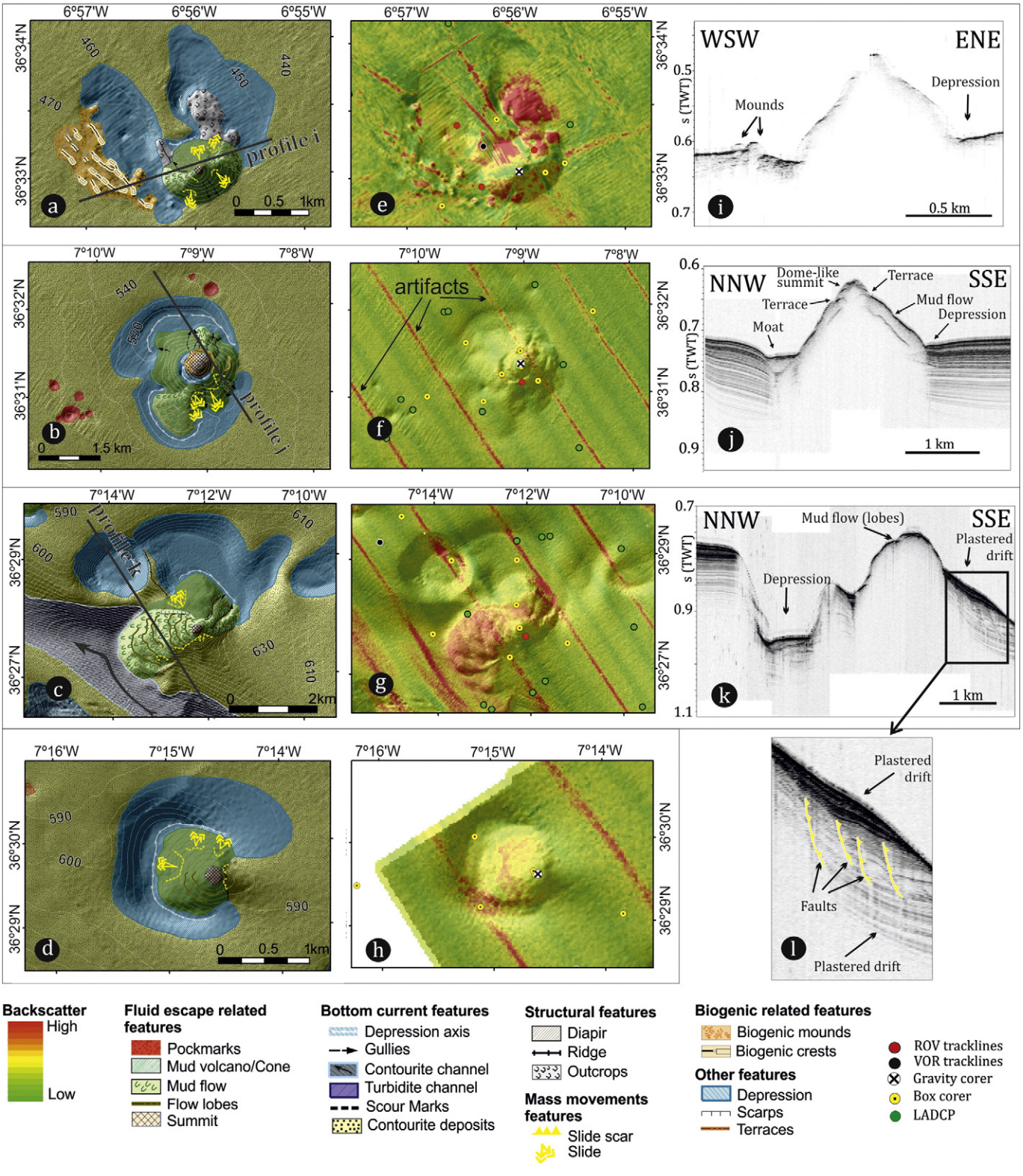

Fig. 2. Main morphological features mapped on the Gazul (a), Anastasya (b), Pipoca (c) and Tarsis (d) MVs, backscatter mosaic maps (e–h) and examples of selected very high-resolution seismic TOPAS profiles (i–l). Morphological and backscatter maps are represented over a hillshade map with a 15 × 15 m grid cell resolution.

north-northeast, where it reaches its maximum depth, and the very high-resolution seismic profiles show parallel reflectors that appear abruptly truncated. The sediment infill reaches a thickness of at least 50 m. In the Huelva channel the reflectors are truncated and the sediment infill is characterised by mud flows from the volcano flanks intercalated between the sandy deposits of the contourite on the channel flank (Fig. 6).

Two box-core samples with 18 cm of sediment thickness were retrieved from the summit of Pipoca MV. The upper 2 cm is composed of light brown hemipelagic sediments that overlie mud breccia facies.

Fauna associated with gas-charged sediments at the summit of the MV include the polychaete *Siboglinum* sp. and the decapod *Calliax* sp. (living individuals collected). Remains of valves of the bivalve *L.*

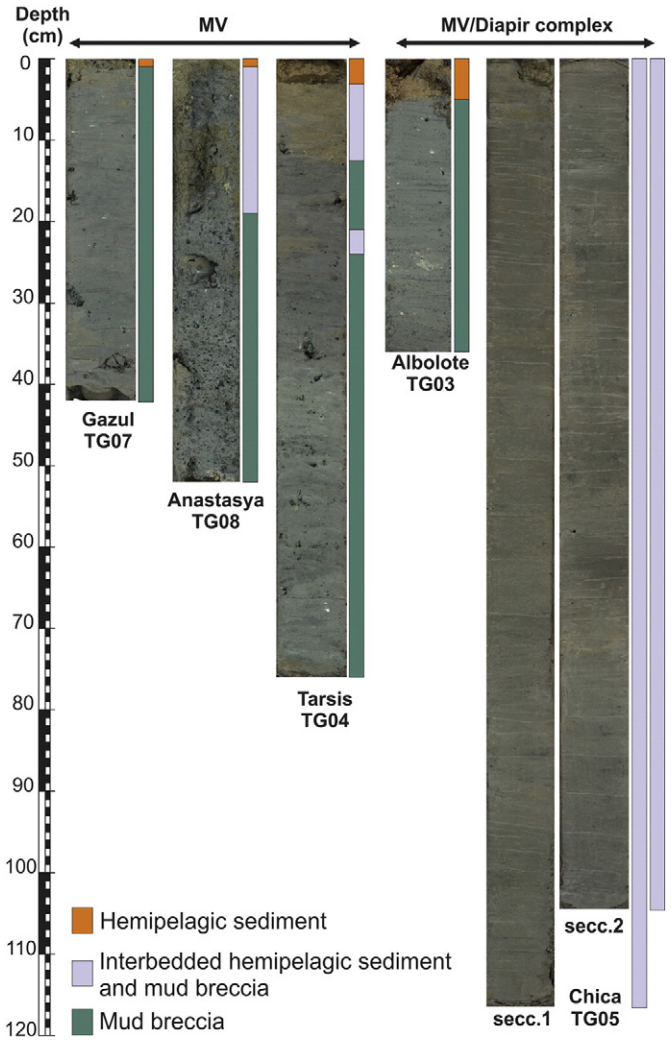

Fig. 3. High-resolution photographs and sedimentary facies identified in the gravity cores retrieved from the summits of mud volcanoes (Gazul, Anastasya, and Tarsis) and MV/diapir complexes (Albolote, Chica). See locations on Fig. 1b.

asapheus were also collected. On the southeastern flank and at the summit of Pipoca MV there are dense crinoid beds of Mediterranean affinity occur (*Leptometra phalangium*) occur (Fig. 4). Disperse authigenic carbonates were observed during the ROV profile.

5.1.4. Tarsis MV

Tarsis mud volcano is situated on the western side of the SFFE, to the west of the Guadalquivir diapiric ridge and to the north of the Huelva channel (Fig. 1). This MV is smaller in size, when compared to the rest of the mud volcanoes considered in this study. The summit located at a water depth of 550 m, has a smooth slope. On the western flank the base reaches 680 m water depth and at the eastern it reaches 590 m water depth, although the mean height is 35 m above the seafloor (Fig. 2d). Therefore has a very asymmetrical bathymetric profile oriented WNW–ESE. The flanks are dominated by mud lobes and slide scars that reach 0.5 km in length on the western side. They have partially dismantled the volcanic edifice, which is covered by contourite deposits on the eastern side. This process is similar to that described for Pipoca MV. The volcanic edifice is surrounded by a moat that reaches a water depth of 100 m. The very high-resolution seismic profiles that cross this depression present deformed reflectors affected by faults that do not reach the surface. The upper layers have reflectors with downlap terminations. Mud flow deposits also fill the base of the depression (Fig. 6).

A 76 cm-long gravity core (TG04) was recovered from the summit of the MV at 550 m water depth (Fig. 3). The top of the recovered material comprises 3 cm of hemipelagic muddy sediments. From 3 cm to 12.5 cm, and from 21 cm to 24 cm, the sedimentary column is characterised by interbedded mud breccia and hemipelagic sand. From 12.5 cm to 21 cm and from 24 cm to the base, the sediment is composed of mud breccia facies. Both, the summit and the zones adjacent to Tarsis MV are characterised by the presence of pennatulaceans (dominated by *Funiculina quadrangularis* and *Kophobelemnon stelliferum*), and the sponge *Thenea muricata*. Very low densities of the polychaete *Siboglinum* sp. have been recorded in the upper levels of the sediment as well as a single specimen of the decapod *Calliax* sp. (Fig. 4).

5.2. Diapirs

5.2.1. Cristobal Colón diapir

This diapir is located in the northwesternmost part of the Guadalquivir diapiric ridge, at water depths of between 389 m and 525 m (Fig. 1). This diapir is tabular in profile view and elongated in a NE–SW direction (Fig. 7a); its semi-major and semi-minor axes are 5.5 and 2.5 km long, respectively. The summit is generally flat, interrupted by small linear depressions and mounds. These mounds have an average height of 10 m and exhibit higher backscatter than the adjacent summit seafloor (Fig. 7e). The main mound, named Isabel de Castilla, is 35 m high and 300 m wide and is located in the eastern region of the summit (Fig. 7a, e). The northern and western base of the diapir is bounded by 15 m deep depressions and two ridges averaging 20 m in height, 0.15 km and 0.2 km in width, and 1.2 km and 2 km in length, respectively. In contrast, the southern flank of the main diapiric structure is characterised by a plastered contourite drift that shows parallel reflectors with onlap terminations, whereas the summit presents a very high amplitude reflector (Fig. 7i).

A box core sample from the Isabel de Castilla mound shows brownish sandy mud sediments with bioclasts and coral rubble that permits us to describe them as carbonate mounds. ROV videos display abundant coral rubble (mainly *M. oculata*, with scarce *L. pertusa*) that is colonised by a wide variety of small gorgonians (*Bebryce*, *Switia* and *Placogorgia*). The southeastern flank is colonised by sea-pens (mainly *F. quadrangularis*, *Pennatula aculeata* and *K. stelliferum*) (Fig. 4).

5.2.2. Juan Sebastian Elcano diapir

This diapir is NE–SW oriented and displays a flat-topped morphology (Fig. 7b), 3 km long and 1.5 km wide. It corresponds to the highest part of the buried Doñana Diapiric Ridge and is located between a water depth of 462 and 556 m. The NW flank has a steep mean slope (around 10°) that terminates in a moat 19 m deeper than the surrounding bottom, whereas the slope angle of the southeastern flank is gentler (4°). The SE flank is characterised by plastered contourite deposits. The diapir raises 94 m on the northwestern flank and 57 m in the southeast. Some small mounded reliefs are observed on the summit although they were not prospected with the ROV. However, the morphological expression and hyperbolic character of the very high-resolution seismic profiles are similar to the carbonate mounds described for the Cristobal Colón diapir (Fig. 7j). In addition, the backscatter values (Fig. 7f) are equivalent to those observed in other edifices in the Gulf of Cádiz where the existence of carbonate mounds has been verified. Two pockmarks situated to the southwest of the edifice have also been mapped (Fig. 7b).

The images and videos of a ROV transect made at the base of the southeastern flank of the diapir show sandy and muddy sediments dominating the bottom. The most abundant species observed with the ROV in some areas of this diapir are pennatulaceans (*K. stelliferum*, *P. aculeata*, and *F. quadrangularis*), with lower numbers of various hydrozoa, sponge and gorgonians species that colonise the hard substrates provided by bioclasts (Fig. 4).

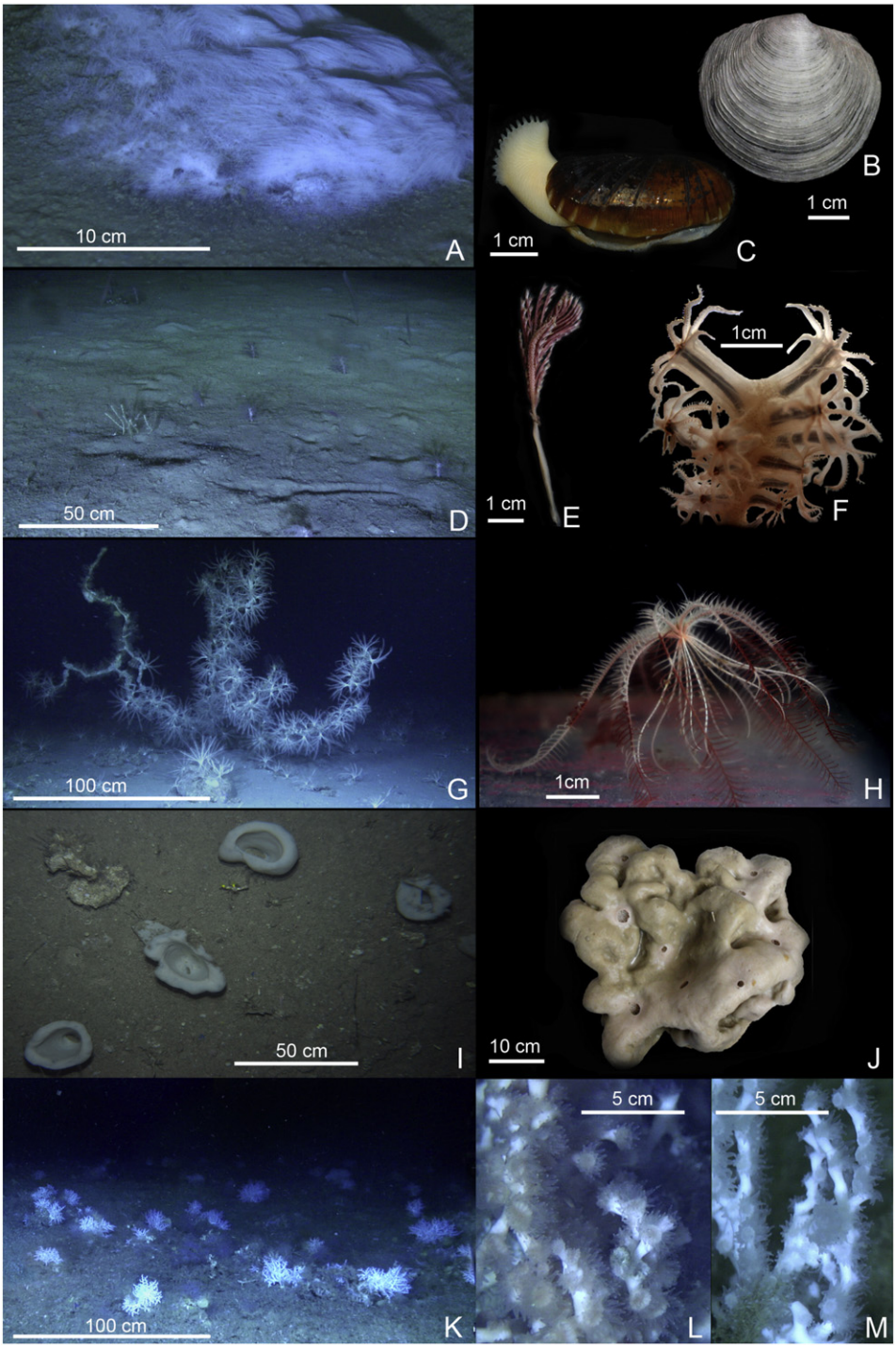

Fig. 4. Examples of some habitats and biological specimens from the Shallow Field of Fluid Expulsion (SFFE). A: Bacterial mats at the summit of Anastasia MV (depth 457 m); B: *Lucinoma asapheus* (chemosymbiotic bivalve); C: *Solemya elarraichensis* (chemosymbiotic bivalve); D: Sea-pen community on the flanks of Anastasya MV (485 m depth); E: *Pennatula aculeata* (Pennatulacea); F: *Kophobelemnon stelliferum* (Pennatulacea); G: Crinoid beds on the southeastern flank of Pipoca MV, colonising sediment, authigenic carbonates, and remains of black corals (530 m depth); H: *Leptometra phalangium* (Crinoid); I: Deep-sea sponge aggregation dominated by *Asconema setubalense* on Enmedio diapir (445 m depth); J: *Petrosia* cf. *crassa* (Porifera); K: Cold-water coral bank dominated by *Madrepora oculata* at Gazul (399 m depth); L: *Lophelia pertusa* (Scleractinian); M: *Madrepora oculata* (Scleractinian).

5.2.3. Enano diapir

Enano is located at the far north end of the Cádiz diapiric ridge, on the western flank of Tofiño channel (Fig. 1). The upward movement of the diapir provides a surface expression of small elongate ridges oriented NNW–SSE (Fig. 7c). The summit of the main ridge is located at 463 m water depth and is elongated in shape with irregular flanks. Very high-resolution seismic profiles reveal several domed seismic units with tilted reflectors that have distal onlap terminations to the diapir that are truncated against the upper discontinuity and have subsequently been filled with the current contourite deposits that characterise this sector of the Gulf of Cádiz (Fig. 7k).

The substrate observed in the underwater imagery is very homogeneous. It is formed by authigenic carbonates such as slabs and chimneys that occupy almost the whole seafloor. These authigenic carbonates are colonised by small sponges, a few antipatharians (*Leiopathes glaberrima*) and mobile fauna such as the echinoids *C. cidaris* and *Echinus* sp., as well

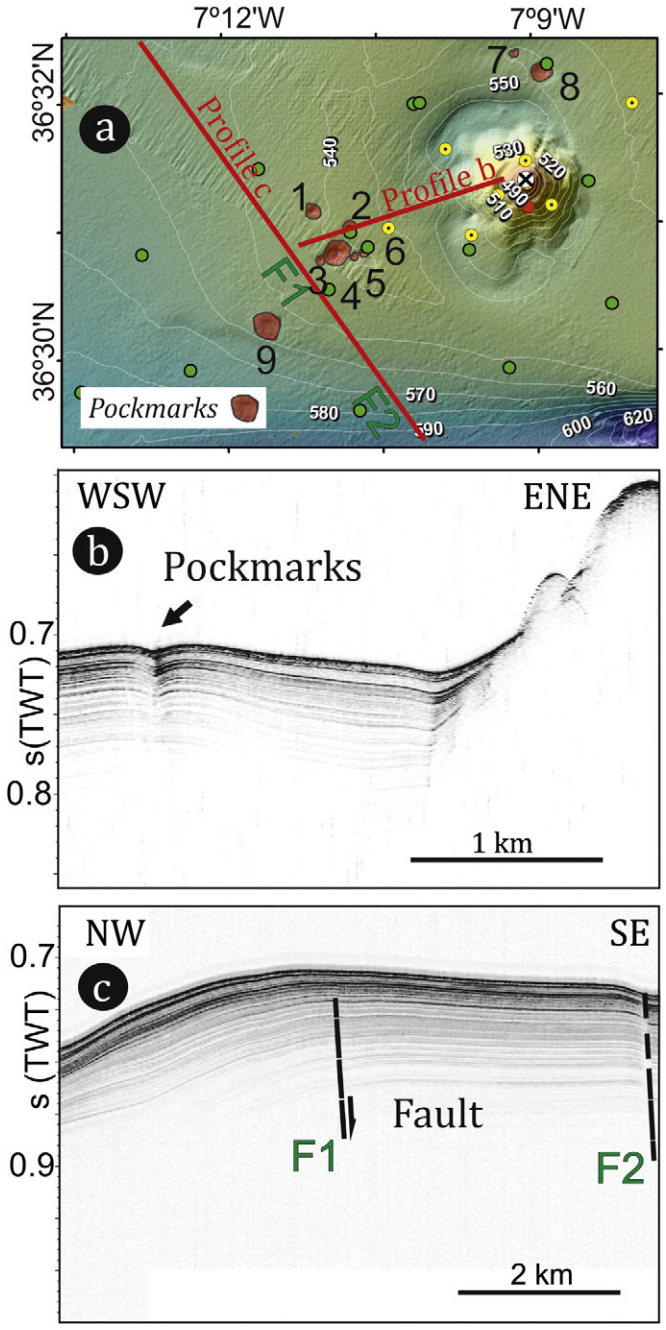

Fig. 5. Example of very high-resolution seismic TOPAS profiles showing pockmarks associated with normal faults.

as the gastropod *Charonia lampas*. The remaining seafloor presents sandy sediments where small ripples (10 cm wavelength) were observed as well as some soft-bottom coloniser including the sponge *T. muricata* (Fig. 4).

5.2.4. Enmedio diapir

Enmedio is located on the Cádiz diapiric ridge between the Gusano and Huelva channels. It has a surface area of 4 km^2, is located at a mean water depth of 440 m, and is bounded by a depression that reaches 630 m water depth to the southwest. A group 10 m-high mound and two cones standing on the base of the surrounding plateau were observed (Fig. 7d). Very high-resolution seismic profiles show deformed reflectors tilted with distal onlap terminations to the diapir that are cut near the upper discontinuity as in the case of Enano diapir. The mounds and cones have a very high amplitude reflector that blocks the seismic signal penetration (Fig. 7l).

The box-core retrieved in the area comprised light brown bioclastic muddy-sand sediments with some gravel-sized lithogenic clasts and coral rubble (mainly of *M. oculata* and *Stenocyathus vermiformis*). Underwater images revealed the presence of a large number of fragmented slabs, crusts and chimneys. In the soft substrates, pennatulaceans such as *F. quadrangularis* and *K. stelliferum* dominate together with the sponge *T. muricata*, whereas the hard substrates are colonised by larger species such as the sponges *Asconema setubalense*, *Phakellia* sp. and *Petrosia* cf. *crassa* or the gorgonian *Callogorgia verticillata*, which provide substrate and shelter for the crinoid *Neocomatella europaea* and the fish *Helycolenus dactylopterus* (Fig. 4).

5.3. MV/diapir complexes

5.3.1. Albolote MV/diapir complex

The Albolote complex, the shallowest diapiric outcrop described in the SFFE, is located in the NW part of this area. This zone is characterised by the presence of several turbidite channels that cross the upper slope from 240 m water depth, in an area where the slope angle is higher than that of in the middle slope. These turbidite channels are oriented ENE–WSW, perpendicular to the bathymetric contours. The Albolote complex is divided by one of the abovementioned channels giving rise to two separate summits (Fig. 8a). To the southern side of the channel, there are four cones, with the main one being located at 347 m water depth. To the north of the channel, the complex displays two elongated cones or ridges, with an ENE–WSW direction, located at water depths of 361 m and 328 m. This complex was sampled with a box-corer and a gravity corer and the results confirm its mud volcano nature (i.e., mud breccia facies). The diapir develops an inflexion in the profile view and very high-resolution seismic profiles show reflectors with downlap termination to the northeast and with onlap termination that end abruptly against the diapir to the southwest (Fig. 8g).

A 36 cm-long gravity core (TG03) was retrieved from the summit at a water depth of 353 m (Fig. 3). The recovered material comprised 5 cm of hemipelagic mud sediments overlying very cohesive mud breccia facies with abundant polygenic clasts. The sediments associated with this complex contain abundant remains of cold-water corals (*M. oculata*, *L. pertusa*, and *Dendrophyllia cornigera*), mollusc shells that are sometimes colonised by hydrozoans (*Lytocarpia*, *Acryptolaria*, and *Sertularella*), small gorgonians (*Bebryce* and *Swiftia*), and octocorals (*Anthomastus* sp.). Several remains of the bivalve *L. asapheus* have also been collected but living cold-seep-related fauna was not found in any of the samples studied. Underwater images showed authigenic carbonates, mainly slabs, as well as echinoids (*C. cidaris*) and burrowing decapods (*Munida* sp.) (Fig. 4). These slabs varied in size and were seen in specific locations where presumably fluid venting occurred.

5.3.2. Chica MV/diapir complex

The Chica complex is located close to the Huelva channel, between the Cádiz diapiric ridge and the Guadalquivir diapiric ridge (Fig. 1), at a water depth of 700 m. It is composed of a series of outcrops grouped into two separate complexes and a main depression to the east that is 50 m deep, 1.1 km long and 0.6 km wide. The summit of the southern complex, Chica1, is at a water depth of 654 m. It is surrounded by 7 smaller cones at between 710 and 660 m water depth. The Chica2 complex is located to the north of Chica1 at 655 m water depth and is composed of an isolated body of lower relief than Chica1. Both complexes are separated by a gully that flows into the moat surrounding the W side of the complex (Fig. 8b). The very high-resolution seismic profiles reveal truncated reflectors in the depression and chaotic to hyperbolic facies on the diapir (Fig. 8h).

One gravity core (TG05) was recovered from the summit of the Chica2 complex (652 m water depth) comprising 221 cm (Fig. 3) of homogeneous and structureless sandy mud that becomes muddy sand to

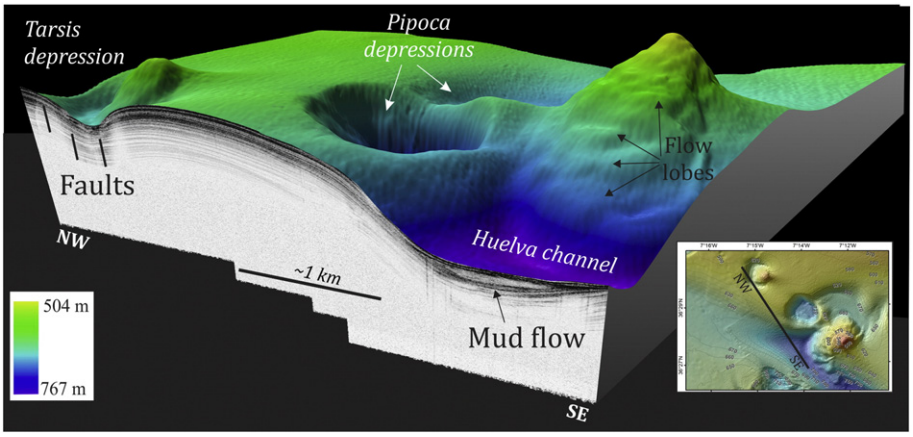

Fig. 6. Block diagram of 3D bathymetric data and very high-resolution seismic profile data from the Tarsis MV and Pipoca MV area.

the base of the core and which smells strongly of hydrogen sulphide. This interbedded facies apparently has no clast except at the top of the core, where a 3 cm thick carbonate crust was observed.

No live individuals or subfossil remains of cold-seep species have been found so far in this complex, but large chimneys and slabs were detected in the ROV images. These chimneys are colonised by large cnidarians (*C. verticillata*, and *L. glaberrima*) and sponges (*A. setubalense*, and *P.* cf. *crassa*). The sandy seafloor is colonised by pennatulaceans and sponges similar to those in other studied areas (Fig. 4).

5.3.3. Magallanes MV/diapir complex

The Magallanes complex is situated on the segment of the Guadalquivir diapiric ridge that is limited to the north by the Gusano contourite channel and to the south by the Huelva contourite channel (Fig. 1). It has a 7.8 km elongated shape oriented SW–NE and is ca. 2 km wide. The summit stands at 407 m water depth and the top is formed by an elongated ridge that runs from the southwest towards the northeast. Several elevations have been observed on the summit that have higher backscatter values than the surrounding seafloor and which are similar to the mounds surveyed in the Cristóbal Colón diapir. They are grouped at the northeast and northwest limits of the ridge summit. The northwestern flank has a steep slope that ends in a depression that reaches a maximum depth of 100 m. This depression is followed by a mounded contourite deposit, whereas the southeast flank of the ridge is covered by plastered contourite deposits that give rise to a gentle slope and therefore make the NW-SE axis asymmetrical in character. A very high-resolution profile shows parallel reflectors in the contourite deposits with up to 60 m of sediment thickness, whereas the summit and northwestern flank have a very high-amplitude reflector (Fig. 8i).

The summit of the complex was sampled with a box-corer that recovered 20 cm of muddy breccias with centimetre-sized clasts and fluidised mud overlain by hemipelagic muddy sands. The dominant species found was the crinoid *L. phalangium*, followed by the scleractinian *F. chunii*, the brachiopod *Gryphus vitreus* and the fish *Helicolenus dactylopterus* and *Chlorophtalmus agassizi*. On the northwestern flank the crinoid *L. phalangium* seems more abundant. At this flank, the substrate contains more authigenic carbonates than at the summit and these are colonised by various species of porifera, echuinoids and crustaceans (Fig. 4).

6. Discussion

The data presented in this study shows that the evolutionary stages of these seepage structures can be buried by the action of the late Quaternary bottom currents and their associated deposits. The main features and habitats (substrate and fauna) observed in this study are linked to two main processes: mud extrusion and fluid seepage, and the interaction with bottom water masses. The seafloor morphology and benthic habitats result from the combination of these processes and establish the key features characterising the environmental conditions at each site. These features can be used to study the evolutive processes of the structures and also enable us to tentatively propose a classification (Fig. 9).

6.1. Mud extrusion and seepage processes

The Gulf of Cadiz is prone to the fluid and gas seepage-related morphologies commonly associated with mud volcanism and mud diapirism, such as: collapse depressions, pockmarks, mud flows, coldseeps, carbonate mounds, and slides (Baraza and Ercilla, 1996; Kenyon et al., 2000; Mazurenko et al., 2002; Pinheiro et al., 2003; Somoza et al., 2002, 2003; Casas et al., 2003; Díaz del Río et al., 2003; Fernández-Puga et al., 2007; León et al., 2010, among others). Some of these features in the SFEE, as well as the new ones described here for the first time, have been described in detail to characterise the natural occurrences of fluid escape and mud extrusion processes in mud volcanoes and diapirs.

The upward migration of muddy sediments and fluids gives rise first to a bulging of the surface (Fig. 9a) and then extrusion of the overpressured material (Fig. 9b). A set of normal hydrostatic faults can develop during the upward migration of fluidised material to the surface. The presence of normal faults around these structures is very common (Fernández-Puga et al., 2007; Medialdea et al., 2009) and they become pathways for fluids to migrate to the surface and/or accumulate sub-seafloor. The stress regime related to the diapiric intrusion and the pore fluid overpressure associated with fluid migration can cause hydraulic faults in the vicinity of the diapir and/or the MV. Wide collapse depressions can be generated as result of the extrusion of large volumes of fluids and gas and also promoted by fault generation or reactivation. This process creates a decrease of interstitial fluid pore pressure and produce large seafloor surface collapses, giving rise to the wide, round-shaped depressions observed in the vicinity of the MVs (Fig. 9c). These are subsequently enlarged by bottom current erosion. This process can also produce the pockmarks that can be seen on the seafloor as small circular shaped depressions.

It has been suggested that large collapse depressions and pockmarks to correspond to similar morphologies at different scales as they are both rounded depressions related to gas expulsion (Somoza et al., 2003; Fernández-Puga et al., 2007). The main difference between them can be observed in high resolution seismic profiles, as pockmarks are generated by a focused fluid migration along faults (Fig. 5) that occurs during mud volcano and diapir emplacement (Prior et al., 1989) without large volumes of accumulated gas (Fig. 9c). The collapse processes may occur during the later stages of the MV evolution as is

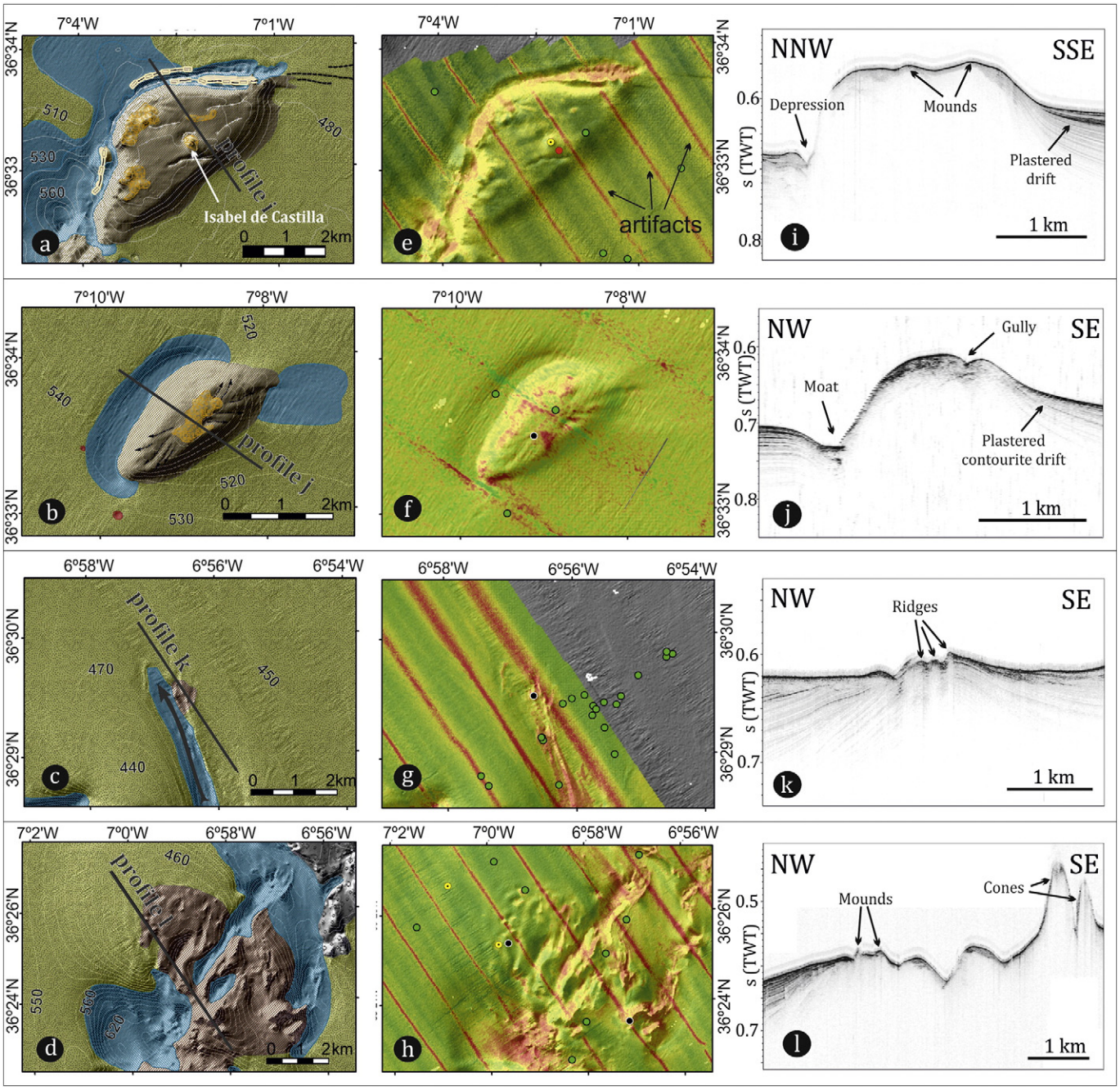

Fig. 7. Main morphological features mapped on the Cristóbal Colón, Juan Sebastián Elcano, Enano and Enmedio diapirs (a–d), backscatter mosaic maps (e–h) and examples of selected very high-resolution parametric TOPAS profiles (e–h). See legend in Fig. 2 for seafloor features. Morphological and backscatter maps are represented over a hillshade map with a 15 × 15 m grid cell resolution.

evidenced by the presence of faults that affect the uppermost Quaternary units. Similar collapse processes have been observed in other mud volcanoes On the Moroccan margin of the Gulf of Cádiz and in the Mediterranean Sea (Van Rensbergen et al., 2005; Camerlenghi et al., 1995).

In the study area, collapse depressions and pockmarks have been identified based on their morphology and by the presence in the seismic profiles of normal faults, truncate reflectors and sediment mixing at the base of these structures. Some of the collapse structures can develop terraces that may be tilted, as is the case of the depression on the main cone of Anastasya MV, which slants to the northwest (Fig. 2j) and the depression at the base of Pipoca MV (Fig. 2k), which tilts to the north-northwest, probably due to post-collapse aggradation. Additionally, these depressions can be affected by current erosion and mass wasting failures. The elongated shape of the eastward depression of Pipoca MV (Fig. 2c) could be explained by the important influence of erosion by the MOW bottom current and its intensification by bottom current eddies and vortex. As well as this, slide deposits have been observed along the walls of the depressions on Pipoca MV.

The development and growth of the mud volcanic edifices occur as a result of active fluid seepage and extrusion of mud flows along the top and flanks of the mud volcanoes (Fig. 9d). In general, mud lobes observed on the flanks of mud volcanoes are related to different episodes of mud flow activity that could indicate different phases in the extrusion process (Van Rensbergen et al., 2005; Kopf, 2002), as has been described for the MVs on the Moroccan margin of the Gulf of Cádiz (León et al., 2012). When mud volcano activity decreases, these mud flow deposits are frequently covered by hemipelagic sediments. Gravity cores recovered at the summit of mud volcanoes in the study area usually display

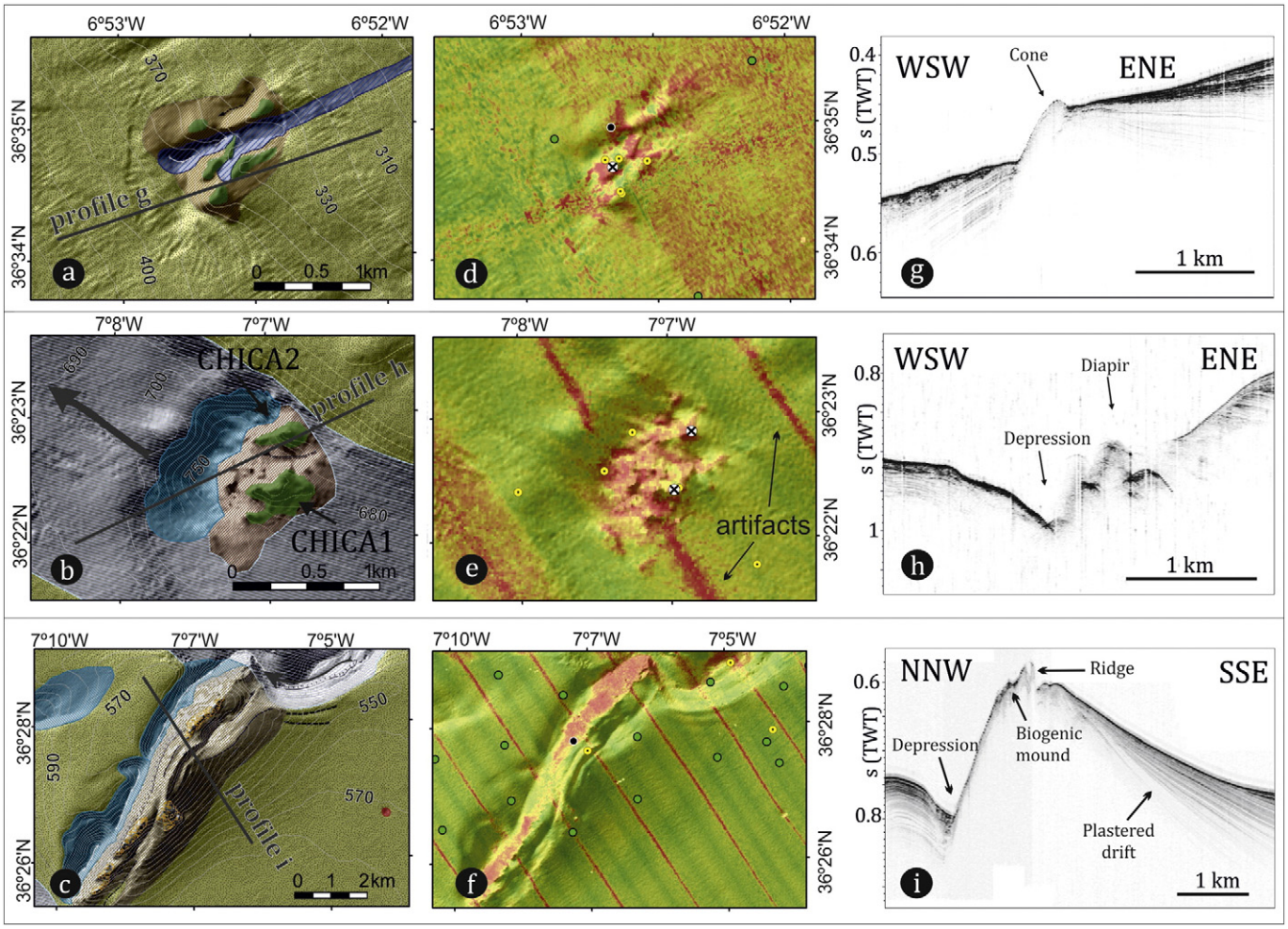

Fig. 8. Main morphological features mapped on the Albolote, Chica and Magallanes MV/diapir complexes (a–c), backscatter mosaic maps (d–f) and examples of selected very high-resolution parametric TOPAS profiles (g–i). See legend in Fig. 2 for seafloor features. Morphological and backscatter maps are represented over a hillshade map with a 15 × 15 m grid cell resolution.

a thin top layer of hemipelagic mud overlying typical mud breccias or a transition zone of interbedded sediments (Fig. 3) indicating alternating periods of mud flow extrusion and quiescence (Kopf, 2002; León et al., 2007). This points to a pulsatile venting process. Seismic facies identified as mud flows appear buried and intercalated with units of subparallel reflectors interpreted as contourite deposits on the SE flank of Pipoca MV (Fig. 2l). This internal structure corroborates the fact that accommodation and different fluid extrusion phases were common processes in Pipoca and Tarsis MVs and could have originated the mud lobes observed on the flanks of these edifices. High backscatter values displayed in the mud flows of Pipoca and Tarsis compared to those observed in Anastasya could be due to a higher content of very cohesive mud sediments or to the occurrence of authigenic carbonate precipitation. Mud flow extrusion usually generates suitable conditions for the characteristic chemosymbiotic-based communities to establish, which are generally located at the summit and closely related to fluid seepage (Fig. 9d). This can be observed on Anastasya MV where the presence of *Siboglinum* sp., endofaunal bivalves, and decapods associated with gas-saturated sediments has been confirmed. Conversely, the deposition of hemipelagic sediments leads to a change in the benthic communities with chemosymbiotic species being replaced by heterotrophic organism, resulting in a decrease in the abundance of cold-seep fauna, as seen on the Pipoca and Tarsis MVs (Fig. 9e).

The abovementioned features have been found on mud volcanoes, as they relate to mud and fluid extrusion, but similar evolutive processes also take place in diapirs (Fig. 9g). The precipitation of authigenic carbonates, associated with anaerobic methane oxidation coupled with sulphate reduction by a consortia of archaea and bacteria, occurs in association with both MVs and mud diapirs (León et al., 2007; González et al., 2009; Magalhães et al., 2012). The authigenic carbonates collected in the study area mainly comprised tabular-shape chimneys, and slab-shaped pavements, which were formed inside the sediments along the flanks of the MVs and diapirs (Fig. 9e). It is worth noticing, that they were collected in zones where the bottom currents are strong enough to remobilise unconsolidated surficial sediments (see discussion below).

6.2. The effects of the bottom currents velocity

During the growth of mud volcanoes and mud diapirs, bottom currents shape the seafloor and control the benthic fauna and the prevailing habitats. Several features related to bottom current activity have been identified, revealing the importance and strength of these currents that shape the seafloor surface. When bottom currents meet an obstacle such as a MV or diapir, their trajectory and acceleration can be altered, increasing their erosive capacity at some points or promoting sedimentation at others (Hernández-Molina et al., 2006; García et al., 2009; Palomino et al., 2011). Therefore, bottom current velocity and direction are the limiting factors that induce the dominant process and the development of bedforms (Stow et al., 2009).

Zones with low-velocity bottom currents (0.01–0.14 m/s) (Díaz del Río et al., 2014) favour the development of benthic communities related

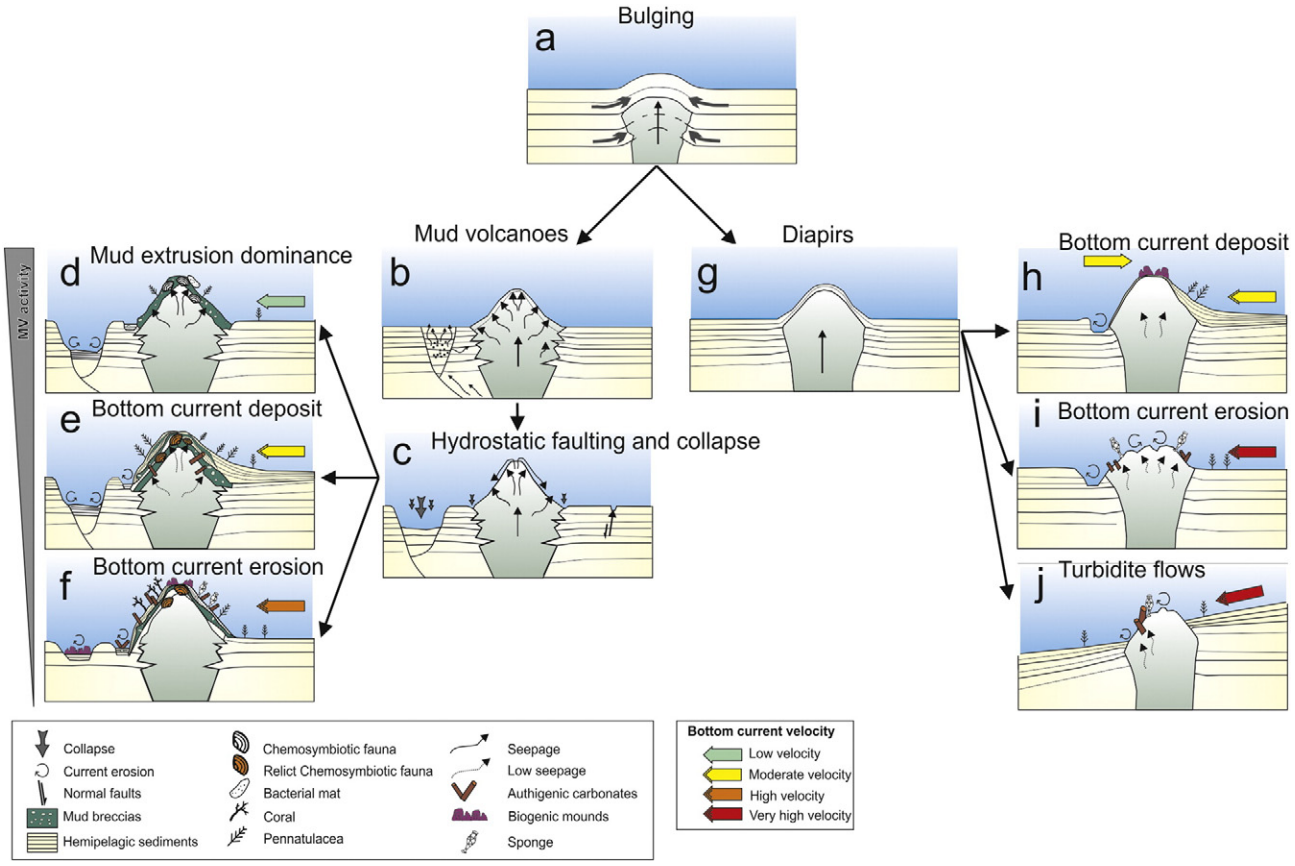

Fig. 9. Stage model showing the various developmental stages of the MVs and diapirs studied in the SFFE, related to mud extrusion and seepage and the prevailing bottom currents.

to seepage. Depositional processes are predominant over erosional processes and collapse depressions may be filled by sediments (Fig. 9d). The best example of these conditions in the study area is observed at Anastasya MV (Fig. 2j) since this structure is exposed to low velocity bottom currents and the sedimentary infill of the collapse depression is 25 m thick with no evidence of erosive processes.

When the bottom current velocity is moderate (0.14–0.21 m/s) (Díaz del Río et al., 2014) plastered contourite deposits develop on the stoss side of the edifices, giving rise to low slope surfaces. This process has mainly been observed on the SE flanks of the MVs (Fig. 9e) and diapirs (Fig. 9h) in the study zone, whereas the opposite flanks of these structures are subjected to erosive processes. These result in an asymmetric geometry of the seafloor, the morphology of which has also been attributed to a displacement of the centres of the mud volcano conduits (León et al., 2012). This may be more noticeable in oval-shaped volcanoes such as Pipoca MV. When these asymmetrical forms are due to contourite sedimentary deposits, the resulting structures signal the bottom current direction.

Another effect of the interaction between bottom currents and the edifices is the increase erosion at the base on the lee side of the structures that initiates the failure structures observed in the high-resolution profiles. This process is evident on the northwestern side of the Pipoca and Tarsis MVs and it could be the trigger mechanism for mass transport deposits at the base of the Pipoca MV collapse depression.

The interaction of the bottom currents with the diapirs generates increased flow speeds and triggers erosion on the lee side of the diapirs that produce the elongated depressions (Fig. 9h). These depressions were defined by García et al. (2009) as marginal valleys formed as consequence of flow instabilities that induced turbulent flows along the NW side of the diapiric ridges.

On the southeastern flank of the Pipoca and Tarsis MVs, overlying the contourite deposits, dense Mediterranean-affinity crinoid beds (*L. phalangium*) occur due to the nature of the water mass (MOW) and the strong hydrodynamism that favours an availability of organic particles for these suspension feeders which are indicative of productive water masses. It is worth noticing that the density of *L. phalangium* in Tarsis MV is less, and the species associated with hard substrates are less abundant (González-García et al., 2012). This change is probably due to the difference in current velocity, as Tarsis MV is located on the lee side of Pipoca MV and could be protected from the strong current (Fernández Salas et al., 2012). The sea-pen communities observed on the flanks of the Cristóbal Colón, Magallanes, and Elcano diapirs may be favoured by the presence of muddy sediments and a moderate current.

The mounds observed on the summit of the diapirs could be carbonate mounds or related biogenic structures, containing hard substrates comprising of coral fragments and benthic fauna within a matrix of hemipelagic sediments. These types of carbonate mounds are very common in the Gulf of Cádiz due to the decline that cold-water corals experienced after the last ice-age (Wienberg et al., 2009). These structures could provide the high backscatter values observed due to their high authigenic carbonate content. Ridges at the northern and western bases of the Magallanes and Cristobal Colon diapirs are related to tectonic scarps that could have been colonised by corals in the past. These features indicate that nowadays the bottom currents may not be able to support living corals (Fig. 9h). The large amount of coral rubble suggests that different oceanographic conditions prevailed in the past, which favoured the growth of carbonate mound, and meant that the water mass provided enough nutrients and a current speed that supported cold-water coral reefs.

When the bottom current velocity is high (0.21–0.3 m/s) there is a predominance of erosive processes. Gazul MV is the only edifice with these conditions in the entire study area (Fig. 9f). Large elongated depressions evidence erosive processes by bottom currents and the very high-resolution seismic profiles show a very high-amplitude reflector

at the surface generated by a lack of unconsolidated sediments. Samples collected in these depressions indicate that the high backscatter values correspond to authigenic carbonates, mainly slabs and chimneys. These structures are not covered by of sediments, pointing to high bottom current velocities. Chimneys and slabs are formed within the sediments and are exhumed and exposed to seawater by the influence of the bottom currents. The exhumation process is probably due to the strong erosive effect of the bottom current as was already proposed for other zones in the Gulf of Cádiz (Magalhães et al., 2012; Viola et al., 2014). Once exposed, the chimneys could lose stability and fall down to the seafloor, as they are sometimes found as broken fragments. The slabs could therefore favour the settlement of colonial suspension feeders (Freiwald and Roberts, 2005; León et al., 2007). Moreover, the presence of abundant large, sessile suspension feeders (e.g. cnidarians and sponges) on the exhumed authigenic carbonates could be encouraged by strong hydrodynamics that promotes a continuous availability of food particles. The presence of large amounts of shell debris and mounds could be also responsible for the high backscatter values observed in this area. The diffractions observed on the mounds in the superficial reflectors of the very high-resolution profiles are similar to those observed in the carbonate mounds of the Moroccan continental margin (Foubert and Henriet, 2009). At present, live corals have not been detected in the depressions and they are only found in specific areas near the summit of Gazul MV. All this evidence supports the idea that the mounds (isolated or grouped) are of biogenic carbonate structures where the slabs behave as a hard substrate on which various benthic organism settled and grew. The mounds were formed consequently by diagenetic processes like carbonate dissolution and precipitation and could have developed as a consequence of coral accumulation. Chimneys and slabs have also been found along the flanks and these are dominated by benthic communities linked to productive waters with cold-water corals (and other sessile organism) that are able to persist in raised zones. The presence of a high-speed current facilitates nutrient distribution and supplies enough food to favour the development and maintenance of the cold water corals and gorgonian communities near the summit (Hovland, 2008).

High velocities bottom currents (0.3–0.5 m/s) (Díaz del Río et al., 2014) erode the superficial hemipelagic layer of sediments that covers the mud diapirs, exhuming the diapiric material. These currents also cause the exhumation of the authigenic carbonates by eroding the unconsolidated sediments. The carbonates are then colonised by sponges and other benthic species. The Enmedio diapir is located over the Tofiño contourite channel where the action of very high-velocity bottom current flows is confirmed by the presence of large number of pavements exhumed as result of the highly erosive effect of the current. ROV imagery shows, in specific areas around the Enano diapir, the development of small ripples, indicating the presence of intensified currents. The Chica complex is located in the course of the Huelva contourite channel and therefore the morphology and characteristics of the edifice are determined by the bottom currents. The large depression mapped in this area was probably caused by erosive processes associated to the high velocity of the MOW that flows along this contourite channel. Again, the formation and exhumation of authigenic carbonates provide a suitable substrate for cnidarians and sponges (Fig. 9i).

The Albolote complex is situated in an area of very high-velocity along-slope currents and is also affected by a down-slope turbidite current, corroborated by the presence of a down-slope channel that crosses the complex (Fig. 9j). These conditions may explain why mud volcanoes are not detected in high velocity areas since bottom currents sweep away the extruded material, impeding the accumulation of mud breccias and the formation of the typical topographic highs of the MV edifices.

6.3. Evidence of the seepage stage

The activity and dynamics of seepage areas can be studied through different factors, including the thickness of the hemipelagic sediments that overlie the mud flow breccias (for mud volcanoes and MV/diapir complexes) and the presence of typical cold-seep fauna, including chemosymbiotic communities. Moreover, the development of benthic communities associated with hard substrates is linked to the presence of authigenic carbonates, which are also indicative of fluid venting not only in MVs, but also in mud diapirs.

The superficial hemipelagic layer overlying the mud breccia sediments observed in the sedimentary column retrieved from the summits of some MVs indicate their activity stage (emission vs. latent conditions) and the thickness of this layer can provide information on the sedimentation since the last sediment extrusion (Van Rensbergen et al., 2005). In general, the thicker this layer is, the longer the period of the inactive phase, although other factors such as the sedimentation rate should be taken into account. For example, this layer is approximately 1 cm thinner on both Anastasya MV and Gazul MV than on the rest of the studied edifices. Anastasya MV seems to be the most active structure in the study area, especially when considering the typical cold seep fauna found at its summit and the characteristics of the mud breccia sediments (the presence of gas bubbles, strong smell of hydrogen sulphide, and mousse-like texture observed in core TG08). Nevertheless, except for the thin hemipelagic layer, there is no other evidence of active seepage processes at present in Gazul MV. This may be due more to the bottom current effect that prevents sediment accumulation and also promotes the presence of the cold-water coral communities observed on this MV.

The benthic chemosymbiotic faunas sampled on Anastasya MV, Pipoca MV and Tarsis MV are quite different. On a MV with active hydrocarbon-rich fluid seepage, the faunas present can be very heterogeneous, with heterotrophic and autotrophic organisms that are directly linked to the seepage, and chemosynthetic bacteria playing an important ecological role (Vanreusel et al., 2009). The species occurring on Anastasya MV, such as the frenulate polychaete *Siboglinum* sp., are generally common dominant components in Gulf of Cádiz cold seeps (Cunha et al., 2013; Rodrigues et al., 2013). Endofaunal communities associated with gas saturated sediments, such as decapod crustaceans of the genus *Calliax* and the chemosymbiotic bivalves *S. elarraichensis* and *L. asapheus*, generally inhabit sediments with low to moderate methane and sulphur emissions (Oliver et al., 2011; Rueda et al., 2012b; Rodrigues et al., 2013; Taviani et al., 2013). Seepage activity on Anastasya MV promotes extremophile conditions of the anoxic sediments, as observed on several MV along the Moroccan continental margin (Vanreusel et al., 2009). The abundance of *Siboglinum* sp. on various volcanoes could also be used as an indicator of the methane availability in the sediments. High densities of *Siboglinum* sp. have been recorded from Anastasya MV (378 indiv/m^2) and lower densities have been seen on Pipoca (<100 indiv/m^2), Gazul (~10 indiv/m^2) and Tarsis (absence of *Siboglinum*) (Rueda et al., 2012b). These values may be used as estimators of the seepage activity, with this being higher at Anastasya than at the Pipoca, Gazul or Tarsis MVs. Moreover, the bacterial mats located at the summit of Anastasya MV are associated with high local fluxes of sulphur formation. On the other hand, remains of the bivalve *L. asapheus* were collected on Gazul MV and in various zones of the Albolote complex. These remains indicate the presence of relict populations that occurred in previous stages of these MVs when seepage was more intense. No live benthic chemosymbiotic fauna have been found in the Chica complex, although the strong smell of hydrogen sulphide in the recovered sediments is indicative of seepage activity. Additionally, the presence of authigenic carbonates could be related to a diffuse seepage flow as has been observed in Gazul MV, Enano diapir, Albolote complex and Chica complex.

7. Conclusions

A multidisciplinary study of several mud volcanoes and mud diapirs has enable correlation to be made between their morphological features and their sedimentary nature, their benthic communities and the

various active sedimentary and oceanographic processes. The main features observed result from a combination of mud extrusion-seepage processes with bottom current effects. Based on this processes, a tentative classification of the mud volcanoes, mud diapirs and mud volcano/diapir morphologies can be proposed (Fig. 9).

There is a good direct correlation between the extrusive activity of the MVs and the abundance of chemosynthesis-based communities, as well as with the presence of collapse depressions and pockmarks near the MV edifices. Besides this, the sampled sediment cores show that the more active the MVs are, the thicker the mud breccia layers. The bottom current effect increases as the seepage activity decreases in intensity, when erosive depressions prevail, authigenic carbonates are exhumed from the sediment and can be colonised hard substrate species, and the benthic fauna changes to species linked to high-productivity water. At the other extreme, there is no evidence of seepage activity at sites where the bottom current velocity is very high. This situation is found in contourite and turbidite channels where erosive processes are predominant.

This classification allows an evolutionary model of the fluid flow structures to be established based on the recognition of their morphological characteristics. This model can be applied to other seepage systems with similar features.

Acknowledgements

This work has been developed as part of the LIFE + INDEMARES/CHICA Project (LIFE07/NAT/E/000732). This work was also a partial contribution to the PAIDI RNM-328 research group. We thank the captains, crews, technicians and scientists aboard the R/V Emma Bardán, R/V Cornide de Saavedra, R/V Ramón Margalef and R/V Vizconde de Eza during the oceanographic cruises. D. Palomino's activities were financed by the Spanish SUBVENT project (CGL2012-39524-C02-01). Two anonymous reviewers and the guest editor Dr. Van Rooij are thanked for constructive comments that served to improve the manuscript.

References

Ambar, I., Howe, M.R., 1979. Observations of the Mediterranean outflow I. Mixing in the Mediterranean outflow. Deep-Sea Res. 26A, 535–554.
Ambar, I., Armi, L., Bower, A., Ferreira, T., 1999. Some aspects of time variability of the Mediterranean water off south Portugal. Deep-Sea Res. I 46, 1109–1136.
Baraza, J., Ercilla, G., 1996. Gas-charged sediments and large pockmark-like features on the Gulf of Cadiz slope (SW Spain). Mar. Pet. Geol. 13 (2), 253–261.
Borenäs, K.M., Wåhlin, A.K., Ambar, I., Serra, N., 2002. The Mediterranean outflow splitting — a comparison between theoretical models and CANIGO data. Deep-Sea Res. II 49, 4195–4205.
Camerlenghi, A., Cita, M.B., Dellavedova, B., Fusi, N., Mirabile, L., Pellis, G., 1995. Geophysical evidence of mud volcanism on the Mediterranean ridge. Mar. Geophys. Res. 17 (2), 115–141.
Casas, D., Ercilla, G., Baraza, J., 2003. Acoustic evidences of gas in the continental slope sediments of the Gulf of Cadiz (E Atlantic). Geo-Mar. Lett. 23 (3/4), 300–310.
Cordes, E.E., Cunha, M.R., Galéron, J., Mora, C., Olu-Le Roy, K., Sibuet, M., Van Gaever, S., Vanreusel, A., Levin, L.A., 2010. The influence of geological, geochemical, and biogenic habitat heterogeneity on seep biodiversity. Mar. Ecol. 31, 51–65.
Criado-Aldeanueva, F., García-Lafuente, J., Vargas, J.M., Del Río, J., Vázquez, A., Reul, A., Sánchez, A., 2006. Distribution and circulation of wáter masses in the Gulf of Cádiz from in situ observations. Deep-Sea Res. II 53, 1144–1160.
Cunha, M.R., Rodrigues, C.F., Génio, L., Hilário, A., Ravara, A., Pfannkuche, O., 2013. Macrofaunal assemblages from mud volcanoes in the Gulf of Cadiz: abundance, biodiversity and diversity partitioning across spatial scales. Biogeosciences 10, 2553–2568.
Davies, T.A., Laughton, A.S., 1972. Sedimentary processes in the North Atlantic. In: Laughton, A.S., Berggren, W.A. (Eds.), Init Rep Deep sea Drilling Project 12. US Government Printing Office, Washington, pp. 905–934.
Dewey, J.F., Helman, M.L., Turco, E., Hutton, D.W.H., Knott, S.D., 1989. Kinematics of the western Mediterranean. In: Coward, M.P., Dietrich, D., Park, R.G. (Eds.), Alpine Tectonics. Geological Society Special Publication 45, pp. 265–283.
Díaz del Río, V., Somoza, L., Martínez-Frías, J., Mata, M.P., Delgado, A., Hernández-Molina, F.J., Lunar, R., Martín-Rubí, J.A., Maestro, A., Fernández-Puga, M.C., León, R., Llave, E., Medialdea, T., Vázquez, J.T., 2003. Vast fields of hidrocarbon-derived carbonate chimneys related to the accretionary wedge/olistostrome of the Gulf of Cadiz. Mar. Geol. 195, 177–200.
Díaz del Río, V., Fernández Salas, L.M., Bruque, G., López-González, F.J., Rueda, J.L., Vázquez, J.T., López, F.J., González-García, E., Palomino, D., Sánchez, O., Oporto, T., Rittierott, C., Rodriguez-Polo, S., Goicoechea, M., Gutiérrez, D., Monroy, F.J., 2012. Emplazamiento de algunas estructuras submarinas relacionadas con la tectónica salina y la expulsión de gases en el talud superior y medio del Golfo de Cádiz. VII Simposio sobre el Margen Ibérico Atlántico, Lisboa, Portugal. Actas proceedings, pp. 121–125.
Díaz del Río, V., Bruque, G., Fernández Salas, L.M., Rueda, J.L., González, E., López, N., Palomino, D., López, F.J., Farias, C., Sánchez, R., Vázquez, J.T., Rittierott, C.C., Fernández, A., Marina, P., Luque, V., Oporto, T., Sánchez, O., García, M., Urra, J., Bárcenas, P., Jiménez, M.P., Sagarminaga, R., Arcos, J.M., 2014. Volcanes de fango del golfo de Cádiz, Proyecto LIFE + INDEMARES. Ed. Fundación Biodiversidad del Ministerio de Agricultura, Alimentación y Medio Ambiente, Madrid (España), pp. 1–128.
Duarte, J.C., Rosas, F.M., Terrinha, P., Schellart, W.P., Boutelier, D., Gutscher, M.-A., Ribeiro, A., 2013. Are subduction zones invading the Atlantic? Evidence from the southwest Iberia margin. Geology 41, 839–842.
Faugères, J.C., Frappa, M., Gonthier, E., De Resseguier, A., Stow, D.A.V., 1985. Modelé et faciès de type contourite a la surface d'une ride sédimentaire édifiée par des courants issus de la veine d'eau méditerranéenne (ride du Faro, Golfe de Cadix). Bull. Soc. Geol. Fr. I 1, 35–47.
Fernández Puga, M.C., Vázquez, J.T., Medialdea, T., Somoza, L., Díaz del Río, V., León, R., 2010. Evidencias morfológicas y geofísicas de la actividad tectónica actual en el sector septentrional del Talud Continental del Golfo de Cadiz. In: Insua, J.M., Martín-González, F. (Eds.), Contribución de la Geología al Análisis de la Peligrosidad Sísmica, pp. 159–162.
Fernández Salas, L.M., Sánchez Leal, R., Rueda, J.L., López González, N., Díaz del Río, V., López Rodríguez, F.J., Bruque, G., Vázquez, J.T., 2012. Interacción entre las masas de agua, los relieves submarinos y la distribución de especies bentónicas en el talud continental del Golfo de Cádiz Geo-Temas 13, p. 198.
Fernández-Puga, M.C., Vázquez, J.T., Somoza, L., Díaz del Río, V., Medialdea, T., Mata, M.P., León, R., 2007. Gas related morphologies and diapirism in the Gulf of Cadiz. Geo-Mar. Lett. 27, 213–221.
Fernández-Puga, M.C., Vázquez, J.T., Sánchez-Guillamón, O., Pajarón, L., Fernández-Salas, L.M., Palomino, D., Díaz del Río, V., 2014. Evidences of contemporary tectonic activity along the Eastern Gulf of Cadiz continental shelf and upper slope (SW Iberian Peninsula). In: Álvarez-Gomez, J.A., Martín-González, F. (Eds.), Una aproximación multidisciplinar al estudio de las fallas activas, los terremotos y el riesgo sísmico, pp. 85–88.
Flinch, J.F., Bally, A.W., Wu, S., 1996. Emplacement of a passive-margin evaporitic allochthon in the Betic Cordillera of Spain. Geology 24 (1), 67–70.
Foubert, A., Henriet, J.P., 2009. Nature and significance of the recent carbonate mound record. Lect. Notes Earth Sci. 126.
Foubert, A., Depreiter, D., Beck, T., Maignien, L., Pannemans, B., Frank, N., Blamart, D., Henriet, J.P., 2008. Carbonate mounds in a mud volcano province off north-west Morocco: key to processes and controls. Mar. Geol. 248 (1–2), 74–96.
Freiwald, A., Roberts, J.M., 2005. Cold-water Corals and Ecosystems. Springer, Heidelberg.
García, M., Hernández-Molina, F.J., Llave, E., Stow, D.A.V., León, R., Fernández-Puga, M.C., 2009. Contourite erosive features caused by the Mediterranean outflow water in the Gulf of Cadiz: Quaternary tectonic and oceanographic implications. Mar. Geol. 257, 24–40.
Gardner, J.M., 2001. Mud volcanoes revealed and sampled on the Western Moroccan continental margin. Geophys. Res. Lett. 28, 339–342.
Gonthier, E.G., Faugeres, J.C., Stow, D.A.V., 1984. Contourite facies of the Faro Drift, Gulf of Cádiz. In: Stow, D.A.V., Piper, D.J.W. (Eds.), Fine-Grained Sediments: Deep Water Processes and Facies. Geol. Soc. Spec. Publ. 15, pp. 275–292.
González, F.J., Somoza, L., Lunar, R., Martínez-Frías, J., Martín Rubí, J.A., Torres, T., Ortiz, J.E., Díaz-del-Río, V., Pinheiro, L.M., Magalhães, V.H., 2009. Hydrocarbon-derived ferromanganese nodules in carbonate-mud mounds from the Gulf of Cadiz: mud-breccia sediments and clasts as nucleation sites. Mar. Geol. 261, 64–81.
González-García, E., Rueda, J.L., Farias, C., Gil Herrera, J., Bruque, G., García Raso, J.E., Fernández-Salas, L.M., Díaz del Río, V., 2012. Comunidades bentónico-demersales en caladeros de los volcanes de fango del golfo de Cádiz: caracterización y actividad pesquera. In: Borja, Á. (Ed.), XVII Iberian Symposium on Marine Biology Studies (SIEBM), San Sebastián - Donostia (Spain). Revista Investigación Marina 19 (6), pp. 377–380.
Gracia, E., Dañobeitia, J., Vergës, J., Bartolomé, R., 2003. Crustal evolution of the Gulf of Cadiz (SW Iberia) at the convergence of Eurasian and African plates. Tectonics 22 (n° 4), 7-1 a–77-19.
Guliyev, I.S., Feizullayev, A.A., 1997. All About Mud Volcanoes. Nafta Press, Baku (52 pp.).
Habgood, E.L., Kenyon, N.H., Masson, D.G., Akhmetzhanov, A., Weaver, P.P.E., Gardner, J., Mulder, T., 2003. Deep-water sediment wave fields, bottom current sand channels and gravity flow channel-lobe systems: Gulf of Cadiz, NE Atlantic. Sedimentology 50, 483–510.
Heezen, B.C., Johnson, G.L., 1969. Mediterranean undercurrent and microphysiography west of Gibraltar. Bull. Inst. Océanogr. Monaco 67 (1382), 1–95.
Hernández-Molina, F.J., Llave, E., Somoza, L., Fernández-Puga, M.C., Maestro, A., León, R., Medialdea, T., Barnolas, A., García, M., Díaz del Río, V., Fernández-Salas, L.M., Vázquez, J.T., Lobo, F., Alveirinho Dias, J.M., Rodero, J., Gardner, J., 2003. Looking for clues to paleoceanographic imprints: a diagnosis of the Gulf of Cádiz contourite depositional systems. Geology 31, 19–22.
Hernández-Molina, F.J., Llave, E., Stow, D.A.V., García, M., Somoza, L., Vázquez, J.T., Lobo, F., Maestro, A., Díaz del Río, V., León, R., Medialdea, T., Gardner, J., 2006. The Contourite Depositional System of the Gulf of Cadiz: a sedimentary model related to the bottom current activity of the Mediterranean Outflow Water and the continental margin characteristics. Deep-Sea Res. II 53, 1420–1463.
Hernández-Molina, F.J., Serra, N., Stow, D.A.V., Llave, E., Ercilla, G., Van Rooij, D., 2011. Along-slope oceanographic processes and sedimentary products around the Iberian margin. Geo-Mar. Lett. 31 (5/6), 315–341.
Hernández-Molina, F.J., Stow, D.A.V., Alvarez-Zarikian, C.A., Acton, G., Bahr, A., et al., 2014a. Onset of Mediterranean Outflow into the North Atlantic. Science 344 (6189), 1244–1250.

Hernández-Molina, F.J., Llave, E., Preu, B., Ercilla, G., Fontan, A., Bruno, M., Serra, N., Gomiz, J.J., Brackenridge, R.E., Sierro, F.J., Stow, D.A.V., Garcia, M., Juan, C., Sandoval, N., Arnaiz, A., 2014b. Contourite processes associated with the Mediterranean Outflow Water after its exit from the Strait of Gibraltar: global and conceptual implications. Geology 42, 227–230.

Hovland, M., 2008. Deep-water Coral Reefs: Unique Biodiversity Hot-spots. Springer/Praxis Publishing, Chichester (278 pp.).

Ivanov, M.K., Kenyon, N., Nielsen, T., Wheeler, A., Monteiro, H., Gardner, J., Comas, M., Akhmanov, A., Akhmetzhanov, G., 2000. Goals and Principal Results of the TTR-9 Cruise. IOC/UNESCO Worksh Rep 168, pp. 3–4.

Johnson, J., Stevens, I., 2000. A fine resolution model of the eastern North Atlantic between the Azores, the Canary Islands and the Gibraltar Strait. Deep-Sea Res. 47, 875–899.

Kenyon, N.H., Ivanov, M.K., Akhmetzhanov, A.M., Akhmanov, G.G., 2000. Multidisciplinary Study of Geological Processes on the North East Atlantic and Western Mediterranean Margins. (Preliminary Results of Geological and Geophysical Investigations During TTR-9 Cruise of R/V Professor Logachev, June–July 1999). IOC/UNESCO Tech Ser 56.

Kopf, A., 2002. Significance of mud volcanism. Rev. Geophys. 40, 1–52.

Lacombe, H., Lizeray, J.C., 1959. Sur le régimedes courants dans le Détroit de Gibraltar. CR Acad. Sci. Paris 248, 2502–2504.

León, R., Somoza, L., Medialdea, T., González, F.J., Díaz-del-Río, V., Fernández-Puga, M.C., Maestro, A., Mata, M.P., 2007. Sea-floor features related to hydrocarbon seeps in deepwater carbonate mud mounds of the Gulf of Cádiz: from mud flows to carbonate precipitates. Geo-Mar. Lett. 27 (2/4), 237–247.

León, R., Somoza, L., Medialdea, T., Hernández-Molina, F.J., Vázquez, J.T., Díaz-del-Río, V., González, F.J., 2010. Pockmarks, collapses and blind valleys in the Gulf of Cádiz. Geo-Mar. Lett. 3, 231–247.

León, R., Somoza, L., Medialdea, T., Vázquez, J.T., González, F.J., López-González, N., Casas, D., Mata, M.P., Fernández-Puga, M.C., Jiménez-Moreno, C.J., Díaz-Del-Río, V., 2012. New discoveries of mud volcanoes on the Moroccan Atlantic continental margin (Gulf of Cadiz): morpho-structural characterization. Geo-Mar. Lett. 32, 473–488.

Llave, E., Hernández-Molina, F.J., Somoza, L., Díaz del Río, V., Stow, D.A.V., Maestro, A., Alveirinho Dias, J.M., 2001. Seismic stacking pattern of the Faro-Albufeira contourite system (Gulf of Cadiz): a Quaternary record of paleoceanographic and tectonic influences. Mar. Geophys. Res. 22, 475–496.

Llave, E., Schönfeld, J., Hernandez-Molina, F.J., Mulder, T., Somoza, L., Díaz del Río, V., Sánchez-Almazo, I., 2006. High-resolution stratigraphy of the Mediterranean outflow contourite system in the Gulf of Cadiz during the Pleistocene: the impact of Heinrich events. Mar. Geol. 226, 241–262.

Llave, E., Hernández-Molina, F.J., Somoza, L., Stow, D.A.V., Díaz del Río, V., 2007. Quaternary evolution of the contourite depositional system in the Gulf of Cadiz. In: Viana, A., Rebesco, M. (Eds.), Economic and Paleoceanographic Importance of Contourites. Geol. Soc. London, Sp. Publ. 276, pp. 49–79.

Llave, E., Matias, H., Hernandez-Molina, F.J., Ercilla, G., Stow, D.A.V., Medialdea, T., 2011. Pliocene–Quaternary contourites along the northern Gulf of Cadiz margin: sedimentary stacking pattern and regional distribution. Geo-Mar. Lett. 31, 377–390.

Louarn, E., Morin, P., 2011. Antarctic intermediate water influence on Mediterranean sea water outflow. Deep-Sea Res. I 932-942.

Madelain, F., 1970. Influence de la topographie du fond sur l'ecoulement Mediterrraneen entre le Detroit de Gibraltar et le Cap Saint-Vincent. Cah. Océanogr. 22, 43–61.

Maestro, A., Somoza, L., Medialdea, T., Talbot, C.J., Lowrie, A., Vázquez, J.T., Díaz-del-Río, V., 2003. Large-scale slope failure involving Triassic and Middle Miocene salt and shale in the Gulf of Cadiz (Atlantic Iberian Margin). Terranova 15, 380–391.

Magalhães, V.H., Pinheiro, L.M., Ivanov, M.K., Kozlova, E., Blinova, V., Kolganova, J., Vasconcelos, C., McKenzie, J.A., Bernasconi, S.M., Kopf, A.J., Díaz-del-Río, V., González, J.F., Somoza, L., 2012. Formation processes of methane-derived authigenic carbonates from the Gulf of Cadiz. Sediment. Geol. 243-244, 155–168.

Maldonado, A., Nelson, C.H., 1999. Interaction of tectonic and depositional processes that control the evolution of the Iberian Gulf of Cadiz margin. Mar. Geol. 155, 217–242.

Maldonado, A., Somoza, L., Pallarés, L., 1999. The Betic orogen and the Iberian–African boundary in the Gulf of Cadiz: geological evolution (central North Atlantic). Mar. Geol. 155, 9–43.

Martín-Puertas, C., Mata, M.P., Fernández-Puga, M.C., Díaz del Río, V., Vázquez, J.T., Somoza, L., 2007. A comparative mineralogical study of gas-related sediments of the Gulf of Cádiz. Geo-Mar. Lett. 27, 223–235.

Matias, H., Kress, P., Terrinha, P., Mohriak, W., Menezes, P.T.L., Matias, L., Santos, F., Sandnes, F., 2011. Salt tectonics in the western Gulf of Cadiz, southwest Iberia. AAPG Bull. 95 (10), 1667–1698.

Mazurenko, L.L., Soloviev, V.A., Belenkaya, I., Ivanov, M.K., Pinheiro, L.M., 2002. Mud volcanoes gas hydrates in the Gulf of Cádiz. Terra Nova 14 (5), 321–329.

Medialdea, T., Vegas, R., Somoza, L., Vázquez, J.T., Maldonado, A., Díaz-del-Río, V., Maestro, A., Córdoba, D., Fernández-Puga, M.C., 2004. Structure and evolution of the "Olistostrome" complex of the Gibraltar Arc in the Gulf of Cadiz (eastern Central Atlantic): evidence from two long seismic cross-sections. Mar. Geol. 209, 173–198.

Medialdea, T., Somoza, L., Pinheiro, L.M., Fernández-Puga, M.C., Vázquez, J.T., León, R., Ivanov, M.K., Magalhaes, V., Díaz-del-Río, V., Vegas, R., 2009. Tectonics and mud volcano development in the Gulf of Cádiz. Mar. Geol. 261, 48–63.

Milkov, A.V., 2000. Worldwide distribution of submarine mud volcanoes and associated gas hydrates. Mar. Geol. 167, 29–42.

Mulder, T., Lecroart, P., Voisset, M., Schönfeld, J., Le Drezen, E., Gonthier, E., Hanquiez, V., Zahn, R., Faugères, J.-C., Hernández-Molina, F.J., Llave-Barranco, E., Gervais, A., 2002. Past deep ocean circulation and the paleoclimate record—Gulf of Cadiz. EOS Trans. Am. Geophys. Union 83 (43), 487–488 (481).

Mulder, T., Voisset, M., Lecroart, P., Le Drezen, E., Gonthier, E., Hanquiez, V., Faugères, J.C., Habgood, E., Hernandez-Molina, F.J., Estrada, F., Llave-Barranco, E., Poirier, D., Gorine, C., Fuchey, Y., Voelker, A., Freitas, P., Lobo Sanchez, F., Fernandez, L.M., Kenyon, N.H., Morel, J., 2003. The Gulf of Cadiz: an unstable giant contourite levee. Geo-Mar. Lett. 23, 7–18.

Mulder, T., Lecroart, P., Hanquiez, V., Marches, E., Gonthier, E., Guedes, J.C., Thiébot, E., Jaaidi, B., Kenyon, N., Voisset, M., Perez, C., Sayago, M., Fuchey, Y., Bujan, S., 2006. The western part of the Gulf of Cadiz: contour currents and turbidity currents interactions. Geo-Mar. Lett. 26, 31–41.

Nelson, C.H., Baraza, J., Maldonado, A., 1993. Mediterranean undercurrent sandy contourites, Gulf of Cadiz, Spain. Sediment. Geol. 82, 103–131.

Nelson, C.H., Baraza, J., Maldonado, A., Rodero, J., Escutia, C., Barber, J.H., 1999. Influence of the Atlantic inflow and Mediterranean outflow currents on Late Quaternary sedimentary facies of the Gulf of Cadiz continental margin. Mar. Geol. 155, 99–129.

Ochoa, J., Bray, N.A., 1991. Water mass exchange in the Gulf of Cadiz. Deep-Sea Res. 38 (1), 465–503.

Oliver, G., Rodrigues, C.F., Cunha, M.R., 2011. Chemosymbiotic bivalves from the mud volcanoes of the Gulf of Cadiz, NE Atlantic, with descriptions of new species of Solemyidae, Lucinidae and Vesicomyidae. ZooKeys 113, 1–38.

Palomino, D., Vázquez, J.T., Ercilla, G., Alonso, B., López-González, N., Díaz del Río, V., 2011. Interaction between seabed morphology and water masses around the seamounts on the Motril Marginal Plateau (Alboran Sea, Western Mediterranean). Geo-Mar. Lett. 31, 465–479.

Pinheiro, L.M., Ivanov, M.K., Sautkin, A., Akhmanov, G., Magalhães, V.H., Volkonskaya, A., Monteiro, J.H., Somoza, L., Gardner, J., Hamouni, N., Cunha, M.R., 2003. Mud volcanism in the Gulf of Cadiz: results from the TTR-10 cruise. Mar. Geol. 3269, 1–21.

Platt, J.P., Behr, W.M., Johanesen, K., Williams, J.R., 2013. The Betic-Rif arc and its orogenic hinterland: a review. Annu. Rev. Earth Planet. Sci. 41, 313–357.

Prior, D.B., Doyle, E.H., Kaluza, M.J., 1989. Evidence for sediment eruption on deep sea floor, Gulf of Mexico. Science 243, 517–519.

Rodero, J., Lobo, F.J., Hernández-Molina, F.J., Somoza, L., Maldonado, A., 2000. Analysis of hummocky morphologies on the upper slope of the Gulf of Cadiz. 3° Simpósio sobre a Margem Ibérica Atlântica, Faro, Portugal. Actas proceedings, pp. 381–382.

Rodrigues, C.F., Hilário, A., Cunha, M.R., 2013. Chemosymbiotic species from the Gulf of Cadiz (NE Atlantic): distribution, life styles and nutritional patterns. Biogeosciences 10, 2569–2581.

Rueda, J.L., González-García, E., Urra, J., Oporto, T., Gofas, S., García-Raso, E., López-González, N., Fernández-Salas, L.M., Díaz del Río, V., 2012a. Chemosymbiotic species associated with mud breccia sediments from mud volcanoes within Spanish waters (Gulf of Cadiz). In: Borja, A. (Ed.), XVII Simposio Ibérico de Estudios de Biología Marina, San Sebastian (España). Revista de Investigación Marina 19 (6), pp. 312–314.

Rueda, J.L., Urra, J., Gofas, S., López-González, N., Fernández-Salas, L.M., Díaz-del-Río, V., 2012b. New records of recently described chemosymbiotic bivalves for mud volcanoes within the European waters (Gulf of Cádiz). Mediterr. Mar. Sci. 13 (2), 262–267.

Sánchez, R., Relvas, P., 2003. Spring-summer climatological circulation in the upper layer in the region of Cape St. Vincent, Southwest Portugal. ICES J. Mar. Sci. 60, 1232–1250.

Schönfeld, J., Zahn, R., 2000. Late glacial to Holocene history of the Mediterranean out flow. Evidence from benthic foraminiferal assemblages and stable isotopes at the Portuguese margin. Palaeogeogr. Palaeoclimatol. Palaeoecol. 159 (85e), 111.

Serra, N., Ambar, I., Käse, R.H., 2005. Observations and numerical modelling of the Mediterranean outflow splitting and eddy generation. Deep-Sea Res. II 52, 383–408.

Somoza, L., Maestro, A., Lowrie, A., 1999. Allochthonous blocks as hydrocarbon traps in the Gulf of Cádiz. Offshore Technology Conference, OTC vol. 10889, pp. 571–577.

Somoza, L., Gardner, J.M., Diaz-del-Rio, V., Vazquez, J.T., Pinheiro, L.M., Hernández-Molina, F.J., the TASYO/Anastasya shipboard parties, 2002. Numerous methane gas-related seafloor structures identified in the Gulf of Cádiz. Eos 83 (47), 541.

Somoza, L., Díaz-del-Río, V., León, R., Ivanov, M., Fernández-Puga, M.C., Gardner, J.M., Hernández-Molina, F.J., Pinheiro, L.M., Rodero, J., Lobato, A., Maestro, A., Vázquez, J.T., Medialdea, T., Fernández-Salas, L.M., 2003. Seabed morphology and hydrocarbon seepage in the Gulf of Cadiz mud volcano area: acoustic imagery, multibeam and ultra-high resolution seismic data. Mar. Geol. 195, 153–176.

Stow, D.A.V., Faugères, J.C., Gonthier, E., 1986. Facies distribution and textural variations in Faro Drift contourites: velocity fluctuation and drift growth. Mar. Geol. 72, 71–100.

Stow, D.A.V., Pudsey, C.J., Howe, J.A., Faugères, J.C., Viana, A.R., 2002. Deep-water contourite systems: modern drifts and ancient series seismic and sedimentary characteristics. Geol. Soc. Lond. Mem. 22.

Stow, D.A.V., Hernández-Molina, F.J., Llave, E., Sayago-Gil, M., Díaz del Rio, V., Branson, A., 2009. Bedform-velocity matrix: the estimation of bottom current velocity from bedform observations. Geology 37, 327–330.

Stow, D.A.V., Hernández-Molina, F.J., Llave, E., Bruno, M., García, M., Díaz del Río, V., Somoza, L., Brackenridge, R.E., 2013. The Cadiz Contourite Channel: sandy contourites, bedforms and dynamic current interaction. Mar. Geol. 343, 99–114.

Taviani, M., Angeletti, L., Ceregato, A., Foglini, F., Froglia, C., Trincardi, F., 2013. The Gela Basin pockmark field in the strait of Sicily (Mediterranean Sea): chemosymbiotic faunal and carbonate signatures of postglacial to modern cold seepage. Biogeosciences 10, 4653–4671.

Thorpe, S.A., 1976. Variability of the Mediterranean undercurrent in the Gulf of Cadiz. Deep-Sea Res. A 23, 711–727.

Van Rensbergen, P., Depreiter, D., Pannemans, B., Moerkerke, G., Van Rooij, D., Marsset, B., Akhmanov, G., Blinova, V., Ivanov, M., Rachidi, M., Magalhaes, V., Pinheiro, L., Cunha, M., Henriet, J.P., 2005. The El Arriache mud volcano field at the Moroccan Atlantic slope, Gulf of Cadiz. Mar. Geol. 219, 1–17.

Van Rooij, D., De Mol, L., Le Guilloux, E., Réveillaud, J., Hernandez-Molina, F.J., Llave, E., Léon, R., Estrada, F., Mienis, F., Moeremans, R., Blamart, D., Vanreusel, A., Henriet, J.P., 2010. Influence of the Mediterranean Outflow Water on benthic ecosystems: answers and questions after a decade of observations. Geo-Temas 11, 179–180.

Vanreusel, A., Andersen, A.C., Boetius, A., Connelly, D., Cunha, M.R., et al., 2009. Biodiversity of cold seep ecosystems along the European margins. Oceanography 22 (1), 118–135.

Vázquez, J.T., Fernández-Puga, M.C., Medialdea, T., Díaz del Río, V., Fernández-Salas, L.M., Llave, E., Lobo, F.J., Lopes, F.C., Maldonado, A., Somoza, L., Palomino, D., 2010. Fracturación normal durante el Cuaternario Superior en la Plataforma Continental Septentrional del Golfo de Cádiz (SO de Iberia). In: Insua, J.M., Martín-González, F. (Eds.), Contribución de la Geología al Análisis de la Peligrosidad Sísmica, pp. 179–182.

Viola, I., Magalhães, V., Pinheiro, L.M., Rocha, F., Capozzi, R., Oppo, D., Terrinha, P., Hensen, C., 2014. Mineralogy and geochemistry of authigenic carbonates from the Gulf of Cadiz. J. Sea Res. 93, 12–22.

Wienberg, C., Hebbeln, D., Fink, H.G., Mienis, F., Dorschel, B., Vertino, A., Correa, M.L., Freiwald, A., 2009. Scleractinian cold-water corals in the Gulf of Cádiz—first clues about their spatial and temporal distribution. Deep-Sea Res. I Oceanogr. Res. Pap. 56 (10), 1873–1893.

Zenk, W., 1975. On the origin of the intermediate double-maxima in T/S profiles from the North Atlantic. Meteor-Forsch. Ergeb. A (16), 35–43.

Zitellini, N., Gràcia, E., Matias, L., Terrinha, P., Abreu, M.A., De Alteriis, G., Henriet, J.P., Dañobeitia, J.J., Masson, D.G., Mulder, T., Ramella, R., Somoza, L., Diez, S., 2009. The quest for the Africa–Eurasia plate boundary west of the Strait of Gibraltar. Earth Planet. Sci. Lett. 280 (1–4), 13–50.